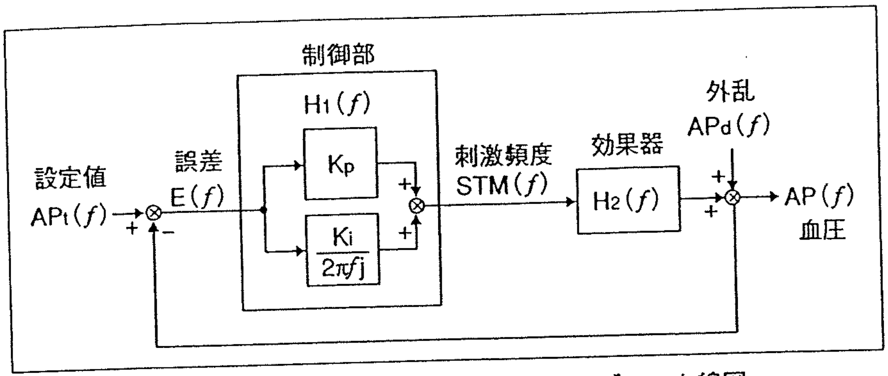

図２ バイオニック動脈圧反射におけるブロック線図
生体本来の動脈圧反射と同様に，バイオニック動脈圧反射では，血圧を乱そうとする外乱の影響を抑制して血圧の安定化をはかる．

動脈圧反射装置を用いたフィードバック制御により，$1/[1+H_1(f)H_2(f)]$に抑制されることがわかる．

以上のようなことから，バイオニック動脈圧反射装置が有効に働くようにするためには，式(2)におけるK_pとK_iが適切に決定されることが必要になる．具体的には，人工的血管運動中枢として働くコンピュータのプログラムが有効性の鍵を握っているということになる．

われわれは，$H_2(f)$を実験的臨床研究によって求め，K_pとK_iについては，数値シミュレーションによってもっとも有効に外乱の影響を抑えることが可能な値に決定し，$H_1(f)$を最適化した．

3．ヒトの交感神経刺激法と刺激に対する血圧の応答特性

これまでの動物実験や臨床研究から，胸腰髄レベルに留置した硬膜外カテーテル電極により，効率よく動脈圧を制御可能であることが判明している6～)8)13)～15)．そこで，変形性頸椎症・頸椎椎間板ヘルニア・後縦靱帯骨化症などの手術時に術中脊髄機能モニタリングとして，脊髄誘発電位記録を行う患者を対象として，不規則に電気刺激を行いながら血圧応答を記録した．12例の患者からデータを取得し，$H_2(f)$を推定した．脊髄の刺激に応じて血圧が変動していることがわかる．

脊髄刺激頻度の変化を入力，血圧応答を出力として推定された伝達関数の結果を図3-Bに示す．平均的な伝達関数$H_2(f)$を求めるために，下記の二次の低域通過フィルターへの曲線近似法を用いて解析した．

$$H_2(f)=\frac{a}{1+2\zeta\left(\frac{f}{f_N}j\right)+\left(\frac{f}{f_N}j\right)^2}\exp(-2\pi fjL)$$

なお，aは定常ゲイン，ζは減衰係数，f_Nは固有周波数，Lはラグ時間である．その結果，それぞれ，0.4, 2.6, 0.06Hz, 9秒という結果が得られた．

4．人工的血管運動中枢の設計

近似$H_2(f)$を用いて，ステップ状の血圧低下(−20mmHg)に対するバイオニック動脈圧反射の振る舞いを比例補償係数$K_p=0, 1, 2$，積分補償係数$K_i=0, 0.01, 0.05, 0.1, 0.2$の組合わせでシミュレーションした．$K_p$と$K_i$の両者が0の場合には，外乱の影響はまったく圧縮されない(図4-A～Cの実線)．

$K_p=0$の場合，全体的に血圧応答が緩徐である．K_iの増加に従い，立上がり時間(rise time, T_r)および整定時間(settling time, T_s)の短縮がみられるが，K_iが0.05を超えると不足減衰応答(underdamped response)がみられるようになり，動脈圧反射が不安定になってくる．

$K_p=2$の場合，T_rは短く応答は迅速であるが，K_iの値にかかわらず動脈圧反射は不安定である．

$K_p=1$の場合，動脈圧反射は，$K_p=0$に比べ迅速で，K_iが0.1になるまでほとんど振動はみられない．$K_i=0.1$のとき，T_rは約50秒で，T_sは60秒以内であった．動脈圧反射の迅速な応答と安定性の両者を満たすものとして，この付近の条件が適していると考えられた．

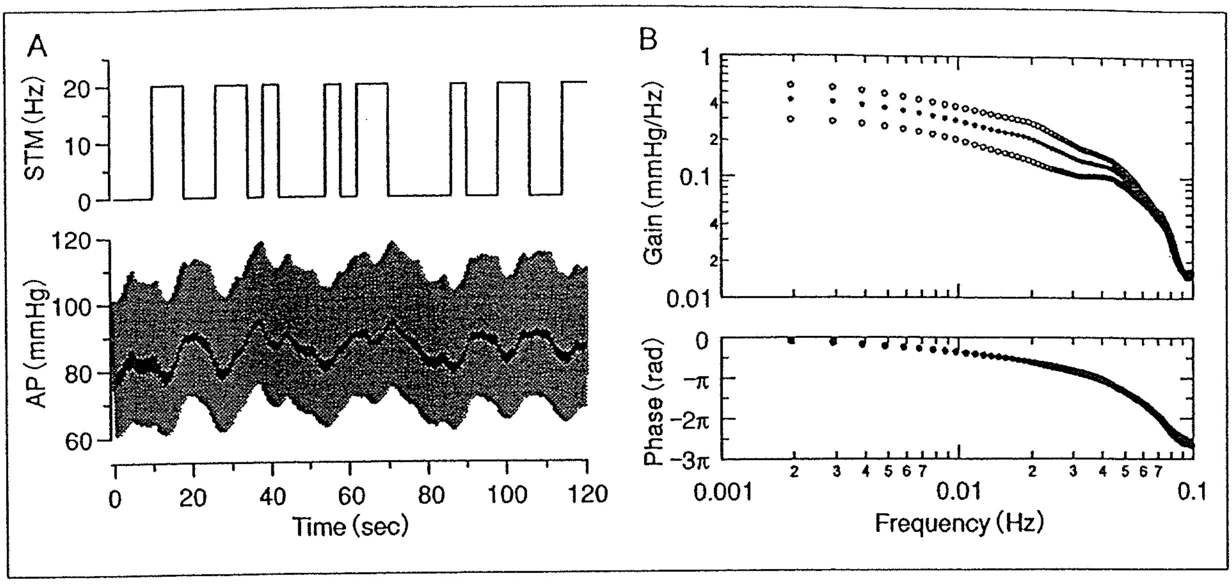

図3
A：不規則な脊髄交感神経刺激に対する血圧応答．刺激頻度(STM)を0か20ヘルツに不規則に変化させ，血圧応答(AP)を記録した．B：刺激頻度の変化に対する血圧応答の動的な特性を示す伝達関数．黒丸が平均値で白丸が平均±標準偏差(12例)を示す．

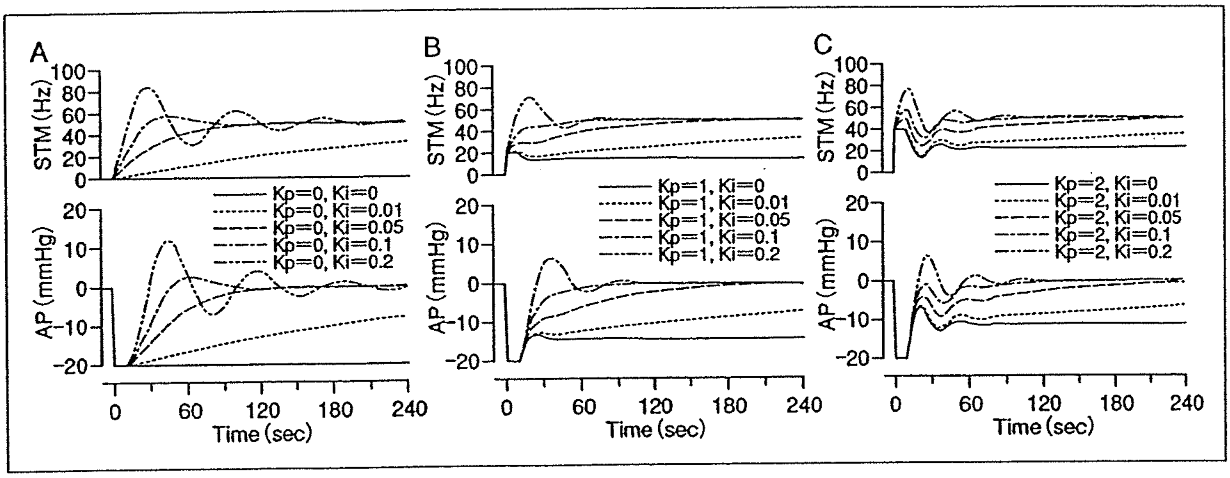

図4　人工的血管運動中枢の設計のためのシミュレーション
図2における比例補償係数(K_p)と積分補償係数(K_i)の組合わせを変えて，−20mmHgの外乱の影響がどのように表れるかを数値解析した．補償係数がともにゼロの場合には，外乱の影響はまったく抑制されない．

バイオニック動脈圧反射装置の有効性の検証

上記の結果を用いて，人工的血管運動中枢を設計し，試作したバイオニック動脈圧反射装置の有効性を検証した．検証にあたっては，起立性低血圧と同様，あるいは類似の血行動態変化による急激でかつ再現性のある低血圧モデルが理想的である．そこで，下肢人工関節置換術の際に止血目的で大腿部に圧迫帯を用いる症例に着目した．このような症例では，圧迫帯の解除時に急激な低血圧を生ずることが知られている16)17)．バイオニック動脈圧反射装置の作動中に圧迫解除を行った場合と，そうでない場合で，血圧がどのように変化するかを検討した．22例から得られた結果は，図5に示されている．大腿部の圧迫止血帯の急速解除に伴う血行動態は，解除後急激に血圧と中心静脈圧が低下した．これは，圧迫解除に伴う下肢への血液貯留により静脈還流が減少し心拍出量が減少したことと，大腿動脈の圧迫解除によって血管床の相対的増加がもたらされ，血管抵抗が減少したことを示

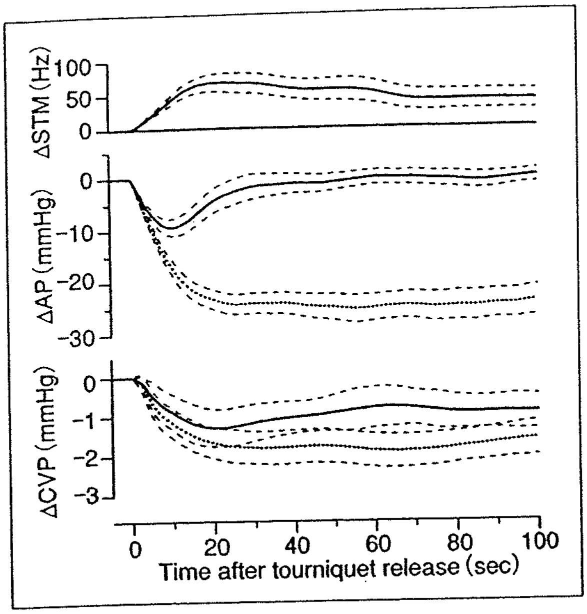

図5　圧迫止血帯の急激な解除に伴う急激な血圧低下
バイオニック動脈圧反射装置が作動していない場合(点線)には，圧迫止血帯の解除に伴い急激に血圧(AP)と中心静脈圧(CVP)が低下したが，バイオニック動脈圧反射が作動している場合(実線)には，両者ともに低下が抑制された．破線は平均±標準偏差(22例)を示す．

唆している．したがって，このような，10秒以内に血圧が20mmHg低下するモデルは，バイオニック動脈圧反射装置の有効性を評価するために妥当であると考えられた．

図から明らかなように，バイオニック動脈圧反射装置が作動している場合には，圧迫止血帯の解除に伴う急激な血圧低下は，数秒以内に食い止められ，止血帯解除前の血圧値にすみやかに回復した．以上のような結果から，バイオニック動脈圧反射装置は，本モデルのような血圧低下に対しては有用であると考えられた．

まとめ

起立性低血圧などのような血圧調節障害に対する治療法として，輸液・輸血法，薬物療法，機械的サポート法などが知られているが，本稿で紹介した手法はこれらとは異なり，自律神経系とインターフェイスして，医工学的に動脈圧反射機能を再建しようとするものである．その利点は，神経性であるがゆえに迅速な調節が可能であるだけでなく，オンデマンド的動作であるため，不要な臥位高血圧をまねく危険性が少ないことも期待される．

バイオニック動脈圧反射装置を臨床応用するにあたっては，長期使用の可能な交感神経刺激電極の開発や小型電気刺激装置が必要となるが，すでに難治性てんかんの治療用としてカフ型の迷走神経刺激電極や刺激装置が開発され，多くの症例に使用されている[18]．したがって，このような要素技術を応用すれば，バイオニック動脈圧反射装置が起立性低血圧の治療器として実用化できるかもしれない．

文　献

1) Robertson D. Diagnosis and management of baroreflex failure. Primary Cardiol 1995 ; 21 : 37.
2) The Consensus Committee of the American Autonomic Society and the American Academy of Neurology. Consensus statement on the definition of orthostatic hypotension, pure autonomic failure, and multiple system atrophy. Neurology 1996 ; 46 : 1470.
3) Ketch T, Biaggioni I, Robertson R, et al. Four faces of baroreflex failure : hypertensive crisis, volatile hypertension, orthostatic tachycardia, and malignant vagotonia. Circulation 2002 ; 105 : 2518.
4) Bannister R, da Costa DF, Hendry WG, et al. Atrial demand pacing to protect against vagal overactivity in sympathetic autonomic neuropathy. Brain 1986 ; 109 : 345.
5) Kristinsson A. Programmed atrial pacing for orthostatic hypotension. Acta Med Scand 1983 ; 214 : 79.
6) Sato T, Kawada T, Shishido T, et al. Novel therapeutic strategy against central baroreflex failure : a bionic baroreflex system. Circulation 1999 ; 100 : 299.
7) Sato T, Kawada T, Sugimachi M, et al. Bionic technology revitalizes native baroreflex function in rats with baroreflex failure. Circulation 2002 ; 106 : 730.
8) Yanagiya Y, Sato T, Kawada T, et al. Bionic epidural stimulation restores arterial pressure regulation during orthostasis. J Appl Physiol 2004 ; 97 : 984.
9) Guyton AC, Coleman TG, Granger HJ. Circulation : overall regulation. Ann Rev Physiol 1972 ; 34 : 13.
10) Sato T, Kawada T, Inagaki M, et al. New analytic

framework for understanding sympathetic baroreflex control of arterial pressure. Am J Physiol Heart Circ Physiol 1999 ; 276 : H2251.
11) Sunagawa K, Sato T, Kawada T. Integrative sympathetic baroreflex regulation of arterial pressure. Ann NY Acad Sci 2001 ; 940 : 314.
12) Kawada K, Sunagawa G, Takaki H, et al. Development of a servo-controller of heart rate using a treadmill. Jpn Circ J 1999 ; 63 : 945.
13) Hainsworth R, Karim F. Responses of abdominal vascular capacitance in the anaesthetized dog to changes in carotid sinus pressure. J Physiol (Lond) 1976 ; 262 : 659.
14) Carneiro JJ, Donald DE. Blood reservoir function of dog spleen, liver, and intestine. Am J Physiol Heart Circ Physiol 1977 ; 232 : H67.
15) Minson CT, Wladkowski SL, Pawelczyk JA, et al. Age, splanchnic vasoconstriction, and heat stress during tilting. Am J Physiol Regul Integr Comp Physiol 1999 ; 276 : R203.
16) Kahn RL, Marino V, Urquhart B, et al. Hemodynamic changes associated with tourniquet use under epidural anesthesia for total knee arthroplasty. Reg Anesth 1992 ; 17 : 228.
17) Sander-Jensen K, Mehlsen J, Secher NH, et al. Progressive central hypovolaemia in man-resulting in a vasovagal syncope? Haemodynamic and endocrine variables during venous tourniquets of the thighs. Clin Physiol 1987 ; 7 : 231.
18) Reid SA. Surgical technique for implantation of the neurocybernetic prosthesis. Epilepsia 1990 ; 31 Suppl 2 : S38.

* * *

Artificial Baroreflex

Clinical Application of a Bionic Baroreflex System

Fumiyasu Yamasaki, MD; Takahiro Ushida, MD; Takeshi Yokoyama, DDS; Motonori Ando, PhD;
Koichi Yamashita, MD; Takayuki Sato, MD

Background—We proposed a novel therapeutic strategy against central baroreflex failure: implementation of an artificial baroreflex system to automatically regulate sympathetic vasomotor tone, ie, a bionic baroreflex system (BBS), and we tested its efficacy in a model of sudden hypotension during surgery.

Methods and Results—The BBS consisted of a computer-controlled negative-feedback circuit that sensed arterial pressure (AP) and automatically computed the frequency (STM) of a pulse train required to stimulate sympathetic nerves via an epidural catheter placed at the level of the lower thoracic spinal cord. An operation rule was subsequently designed for the BBS using a feedback correction with proportional and integral gain factors. The transfer function from STM to AP was identified by a white noise system identification method in 12 sevoflurane-anesthetized patients undergoing orthopedic surgery involving the cervical vertebrae, and the feedback correction factors were determined with a numerical simulation to enable the BBS to quickly and stably attenuate an external disturbance on AP. The performance of the designed BBS was then examined in a model of orthostatic hypotension during knee joint surgery ($n=21$). Without the implementation of the BBS, a sudden deflation of a thigh tourniquet resulted in a 17±3 mm Hg decrease in AP within 10 seconds and a 25±2 mm Hg decrease in AP within 50 seconds. By contrast, during real-time execution of the BBS, the decrease in AP was 9±2 mm Hg at 10 seconds and 1±2 mm Hg at 50 seconds after the deflation.

Conclusions—These results suggest the feasibility of a BBS approach for central baroreflex failure. **(*Circulation*. 2006; 113:634-639.)**

Key Words: baroreceptors ■ blood pressure ■ computers ■ electrical stimulation ■ nervous system, sympathetic

The arterial baroreflex acts to maintain cerebral perfusion by quickly attenuating the effect of an external disturbance, such as the assumption of an upright position, on arterial pressure (AP).[1–4] Therefore, functional restoration of dynamic properties of the arterial baroreflex is essential for the treatment of patients with various syndromes of baroreflex failure,[5] including Shy-Drager syndrome,[6–9] baroreceptor deafferentation,[10,11] and traumatic spinal cord injuries.[12,13] However, most commonly used interventions, including salt loading,[14,15] cardiac pacing,[16,17] and adrenergic agonists,[18,19] can neither restore nor reproduce the functioning of the native vasomotor center, and most affected patients remain bedridden.

Clinical Perspective p 639

We recently developed a framework for identifying an operational rule of the vasomotor center and a prototype of a bionic baroreflex system (BBS) in rats.[20–22] The BBS consisted of a negative-feedback system controlled by a computer (ie, the artificial vasomotor center) that sensed AP and automatically computed the frequency of a pulse train required to stimulate sympathetic efferent nerves through a pair of wire electrodes placed in the celiac ganglion. Previous experimental work demonstrated that the BBS restored native baroreflex function in rats with central baroreflex failure; however, an applicable neural interface with quick and effective controllability of AP is required for application of this technology in the clinical setting. The goal of the present study was to determine the efficacy of a novel bionic technology for the intraoperative restoration of AP in the context of central baroreflex failure and to validate this technology in a clinical model of orthostatic hypotension.

Methods

All studies were approved by the institutional review committee, and all subjects gave informed consent.

Theoretical Considerations

As previously described,[20–22] the principle of the BBS is based on a negative-feedback mechanism (Figure 1). The instantaneous AP is measured by a pressure transducer connected to a computer that functions as a controller or artificial vasomotor center. Instead of the disabled native vasomotor center, the controller automatically exe-

---

Received September 8, 2005; revision received October 31, 2005; accepted November 21, 2005.

From the Departments of Cardiovascular Control (F.Y., M.A., T.S.), Clinical Laboratory (F.Y.), Orthopedic Surgery (T.U.), and Anesthesiology (T.Y., K.Y.), Kochi Medical School, Nankoku, Japan.

Correspondence to Fumiyasu Yamasaki, MD, Department of Clinical Laboratory, Kochi Medical School, Nankoku 783-8505, Japan. E-mail yamasakf@med.kochi-u.ac.jp

Circulation is available at http://www.circulationaha.org

DOI: 10.1161/CIRCULATIONAHA.105.587915

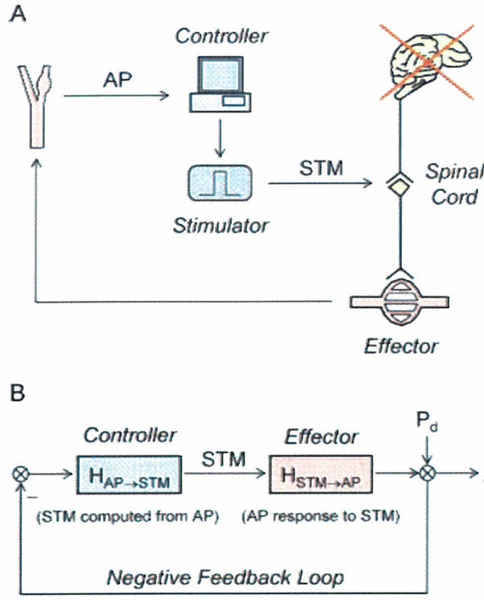

Figure 1. Schematic illustration (A) and block diagram (B) of a BBS. In the context of central baroreflex failure, the BBS automatically computes the frequency (STM) of a pulse train to stimulate sympathetic nerves through an epidural catheter placed at the level of lower thoracic spinal cord, while simultaneously sensing the change in AP. $H_{AP\rightarrow STM}$ denotes a transfer function for the controller functioning as an artificial vasomotor center. $H_{STM\rightarrow AP}$ is a transfer function showing the dynamic response of AP to STM. The overall transfer function of the BBS is given by $H_{AP\rightarrow STM}\times H_{STM\rightarrow AP}$. Therefore, the effect of an external disturbance (P_d) on AP is attenuated to $1/(1+H_{AP\rightarrow STM}\times H_{STM\rightarrow AP})$.

cutes real-time operations that determine the frequency of electrical stimulation (STM) required to minimize the effect of an external disturbance (P_d) on AP and then commands an electrical stimulator to deliver a stimulus of the same frequency to the vasomotor sympathetic nerves via epidural-catheter electrodes placed at the lower thoracic level of the spinal cord. The lower thoracic level was selected as the site for the neural interface of the BBS because the abdominal splanchnic vascular bed is a major effector mechanism for the arterial baroreflex.[23–25]

According to a classic feedback-control theory, ie, feedback correction with proportional and integral gain factors,[26,27] the following algorithm was used to program the controller for the calculation of STM in the frequency domain:

$$H_{AP\rightarrow STM}=K_p+\frac{K_i}{2\pi fj} \tag{1}$$

where $H_{AP\rightarrow STM}$ is a transfer function from AP to STM, K_p is the proportional correction factor, K_i is the integral correction factor, and *j* is the imaginary unit. The proportional factor determines the feedback amplification based on the absolute value of the instantaneous control error due to P_d, and the integral factor adjusts the feedback amplification based on the cumulative value of the instantaneous control error. Therefore, STM is computed as follows:

$$STM=-AP\cdot H_{AP\rightarrow STM} \tag{2}$$

and AP is also expressed as follows:

$$AP=STM\cdot H_{STM\rightarrow AP}+P_d \tag{3}$$

where $H_{STM\rightarrow AP}$ denotes the frequency response of AP to STM. From Equations 2 and 3, the effect of P_d on AP is estimated as follows:

$$AP=\frac{1}{1+H_{AP\rightarrow STM}\cdot H_{STM\rightarrow AP}}P_d \tag{4}$$

Thus, if $H_{AP\rightarrow STM}\cdot H_{STM\rightarrow AP}$ is far larger than unity, the BBS can nullify the effect of P_d on AP.

Subjects and Experimental Protocols

A total of 33 patients (46 to 84 years old, 19 males) who underwent orthopedic operations were enrolled in the present study. Ten patients had hypertension, and 4 had diabetes mellitus. None of the subjects had frequent ectopic beats or atrial fibrillation. After induction anesthesia with propofol, an endotracheal tube was introduced orally. The patients were mechanically ventilated with 67% nitrous oxide and 1.5% to 2% end-tidal sevoflurane in oxygen during experimental protocols, while end-tidal carbon dioxide was maintained at 35 to 38 mm Hg. An arterial catheter was placed in the radial artery for AP measurement. To record central venous pressure (CVP), a central venous catheter was placed in the femoral vein, and the tip of the catheter was advanced into the inferior vena cava just above the diaphragmatic level. Furthermore, an epidural catheter was placed percutaneously, and the tip, which contained a pair of electrodes (Unique Medical, Tokyo; interelectrode distance 15 mm), was placed at the level of Th_{9-11}. Placement of the central venous catheter and the epidural catheter was verified by chest radiograph.[28]

Before making an incision of affected areas, we performed 2 different protocols in separate groups of patients. In the first group of patients (n=12, 46 to 76 years old, 7 males) undergoing operations for cervical spondylosis and canal stenosis, the averaged $H_{STM\rightarrow AP}$ was estimated and the $H_{AP\rightarrow STM}$ was designed parametrically with Equation 1 to minimize the effect of P_d on AP. After we programmed the designed $H_{AP\rightarrow STM}$ into the computer, the efficacy of the BBS was tested against the rapid progressive hypotension induced by use of a thigh tourniquet[29–31] in the second group of patients (n=21, 64 to 84 years old, 12 males) undergoing operation for knee joint osteoarthritis. During each protocol, the muscle twitches induced by spinal cord stimulation were prevented by the intravenous administration of vecuronium bromide. Analgesia for the pain provoked by spinal cord stimulation and tourniquet inflation was provided by intravenous injection of fentanyl citrate. In a preliminary study, the validity of the analgesic preparation was confirmed for the experimental protocols, and the safety of spinal cord stimulation for 20 minutes was verified.

Estimation of Transfer Function From STM to AP

To characterize the dynamic nature of the AP response to STM, ie, $H_{STM\rightarrow AP}$, the lower thoracic sympathetic nerves were randomly stimulated for 15 minutes while we recorded AP. According to a white noise method for system identification, the STM was altered between 0 and 20 Hz every 4 seconds. The pulse width of electrical stimuli was fixed at 0.1 ms. The stimulation current was adjusted for each patient so as to produce a pressor response of ≈10 mm Hg at 20 Hz. This resulted in an average current of 15±4 (mean±SD) mA. The electrical signals of STM and AP were digitized at 100 Hz. As described previously,[20–22] the transfer function from STM to AP, $H_{STM\rightarrow AP}$, was estimated with a fast Fourier transform algorithm. Finally, the average of $H_{STM\rightarrow AP}$ among 12 patients was calculated.

Design of Artificial Vasomotor Center

With substitution of the averaged $H_{STM\rightarrow AP}$ for Equation 4, the instantaneous AP response to P_d was simulated numerically, and a stepwise decline with an amplitude of 20 mm Hg was imposed on the BBS. While the feedback parameters of $H_{AP\rightarrow STM}$, ie, K_p and K_i, were altered, the effect of the parameters on the AP response was investigated. Finally, the parameters that enabled the BBS to quickly and stably minimize the effect of P_d on AP were determined.

Efficacy of BBS in a Clinical Model of Transient Hypotension

The performance of the BBS was evaluated in a clinical model of rapid transient hypotension (n=21). Rapid hypotension was evoked by the sudden deflation of a thigh tourniquet, which is widely used to achieve bloodless dissection during total knee arthroplasty.[29–31] Acute hypotension immediately after tourniquet release is a well-

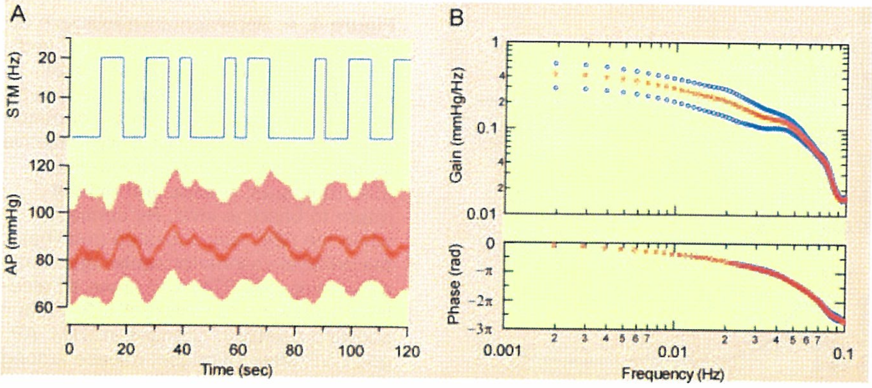

Figure 2. A, Representative example of time series data of the response of AP to random stimulation of the lower thoracic spinal cord. According to quasi-white noise, the STM was randomly altered between 0 and 20 Hz. The AP seems to slowly respond to STM with a delay. B, Transfer function of the AP response to the STM change. Data are expressed as mean±SD for 12 patients. rad indicates radians. See text for explanation.

known phenomenon that results from a rapid decrease in peripheral vascular resistance and an increase in venous pooling in the affected limb.[29] The degree of hypotension can be potentiated by the use of volatile anesthetic agents such as sevoflurane, which are central depressants of arterial baroreflex function.[32,33] Therefore, tourniquet-related hypotension during sevoflurane anesthesia can be used as a model of orthostatic hypotension in central baroreflex failure.

Briefly, a tourniquet was applied to the upper femur and inflated at 300 mm Hg for 60 minutes and then quickly deflated for 10 minutes. The procedure was then repeated. The BBS was activated during 1 of the 2 trials of tourniquet-related hypotension, and the electrical signals of STM, CVP, and AP were digitized at 100 Hz.

Statistical Analysis

The hemodynamic responses to tourniquet release were measured for each subject while the BBS was being activated and inactivated. The effects of the BBS execution on the hemodynamic changes at 10, 50, and 100 seconds after tourniquet release were analyzed by paired *t* tests with Bonferroni adjustment. Differences were considered significant at overall $P<0.05$.

Results

A representative example of original tracings of STM and AP during random stimulation of the spinal cord is shown in Figure 2A. Random on-off change in STM produced a delayed and slow change in AP. The relationship between STM and AP was quantitatively characterized by the frequency domain analysis (Figure 2B). The averaged transfer function from STM to AP, $H_{STM \rightarrow AP}$, had low-pass characteristics with a corner frequency of 0.06 Hz. The gain factor was 0.43 ± 0.13 mm Hg · Hz^{-1} at the steady state (lowest frequency) and gradually decreased with input frequency. The phase spectrum showed that the input-output relationship was in phase and that the phase delay increased toward higher frequencies. The squared coherence, a measure of linear dependence between STM and AP, was >0.9 in the frequency range of interest (data not shown).

The results of simulation for the design of the artificial vasomotor center, $H_{AP \rightarrow STM}$, are presented in Figure 3. The AP responses to the external disturbance P_d were simulated under 12 different combinations with feedback correction factors. Without feedback compensation, ie, when both feedback correction factors were zero, there was no attenuation of the effect of the external disturbance on AP. Therefore, AP fell by 20 mm Hg immediately after the imposition of P_d (Figure 3A, black line). By contrast, if either or both of the correction factors were too large, the underdamped oscillatory response of AP appeared, and the BBS became unstable. On the basis of these results, K_p was set at 1, and K_i was set at 0.1, so that the BBS could quickly and effectively attenuate the effect of the external disturbance (Figure 3B, red line).

A representative example of the results of the performance tests of the BBS is shown in Figure 4A. A sudden

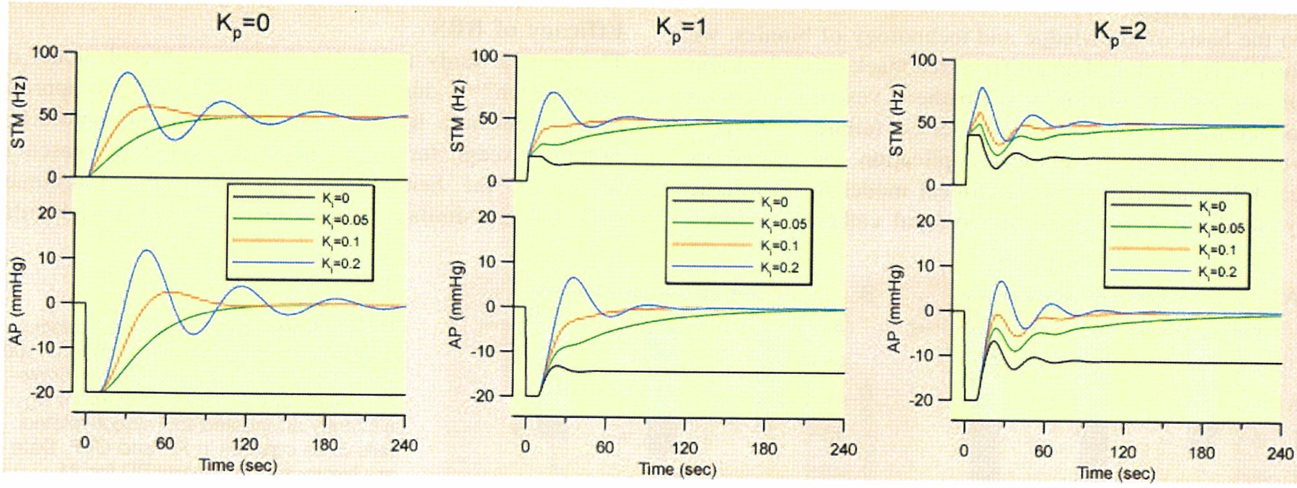

Figure 3. Numerical simulations of a feedback controller of the BBS. A stepwise pressure decline with an amplitude of 20 mm Hg is assumed to be imposed. Results are shown for 12 combinations of proportional (K_p) and integral (K_i) correction factors. See text for explanation.

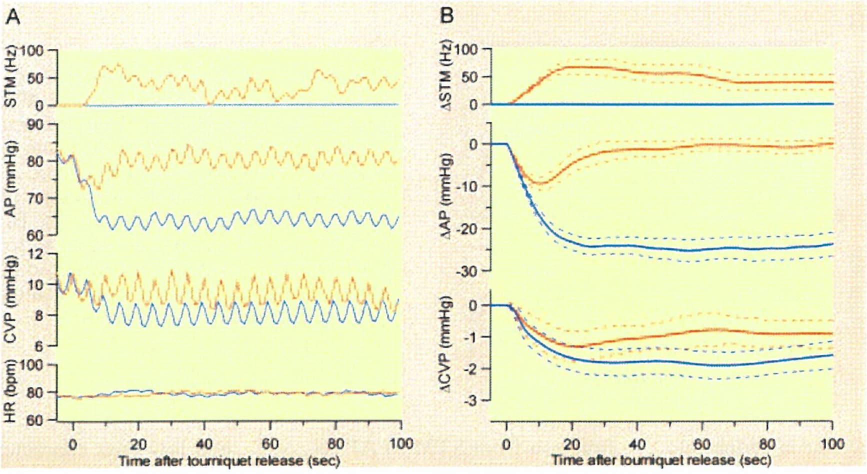

Figure 4. A, Representative example of original tracings of STM, AP, CVP, and heart rate (HR) during 2 episodes of rapid progressive hypotension induced by sudden deflation of a thigh tourniquet in a patient. When the BBS was inactive (blue line), AP decreased immediately after tourniquet release and did not return to baseline level. By contrast, when the BBS was activated (red line), the artificial vasomotor center automatically computed STM and drove an electrical stimulator to restore AP. B, Plots showing averaged changes in STM, AP, and CVP after tourniquet release among 21 patients. Data are expressed as mean (solid line)±SD (dotted line). See text for explanation.

deflation of the thigh tourniquet produced a rapid progressive fall in AP of ≈20 mm Hg within 10 seconds, while lowering CVP by 2 mm Hg. By contrast, when the BBS was activated, STM was computed automatically, and the spinal cord was stimulated appropriately to quickly and effectively attenuate the drop in AP and CVP. Figure 4B summarizes the results obtained from 21 patients, demonstrating effectiveness of the BBS performance in buffering the AP fall in response to the sudden release of the tourniquet. As demonstrated in Figure 5, tourniquet release resulted in an AP decrease of 17±3 mm Hg at 10 seconds, 25±2 mm Hg at 50 seconds, and 24±3 mm Hg at100 seconds. By contrast, during real-time execution of the BBS, the decrease in AP was 9±2 mm Hg at 10 seconds, 1±2 mm Hg at 50 seconds, and 0±1 mm Hg at 100 seconds after the deflation. These data indicated that the BBS significantly attenuated the decrease in AP at these 3 time points and nullified the hypotensive effect of tourniquet release within 50 seconds. Similarly, the BBS significantly suppressed the decrease in CVP within 50 seconds after the release of the tourniquet.

Discussion

Design of BBS

On the basis of knowledge and technology of bionics, we previously developed an artificial feedback control system for automatic regulation of sympathetic vasomotor tone in animal models of central baroreflex failure.[20–22] As a crucial first step to clinical application, we tested its feasibility and efficacy in a clinical model of orthostatic hypotension. A percutaneous epidural catheter approach was established for the monitoring of spinal function during surgery and for pain management,[28] and the lower thoracic level was selected for spinal cord stimulation based on earlier reports that the abdominal splanchnic vascular bed is a major effector mechanism for arterial baroreflex in animals[23,24] and humans.[25] Although the percutaneous epidural approach is less invasive than implantation surgery, spinal cord stimulation excites motor and sensory nerves[12,22,28] in addition to sympathetic vasomotor efferents. Therefore, administration of sufficient doses of muscle relaxants and analgesics was required during experimental protocols. Under these conditions, the dynamic response of AP to STM was easily characterized by the white noise system identification method. Furthermore, the quantitatively estimated results of transfer function analysis (Figure 2B) enabled simulation of the effects of feedback correction factors[27] on performance of the BBS. As demonstrated in Figure 3, the simulation results suggested that the specific combination of feedback correction factors could optimize the performance of the BBS. On the basis of these results, the feedback correction factors were determined to allow the BBS to quickly stabilize AP against the external disturbances.

Efficacy of BBS

The present study utilized a tourniquet-related model of hypotension[29–31] during general anesthesia[32,33] to approximate orthostatic hypotension due to central baroreflex failure. Except for the change in peripheral vascular resistance, the hemodynamic changes after tourniquet deflation are similar to those achieved after upright tilt-

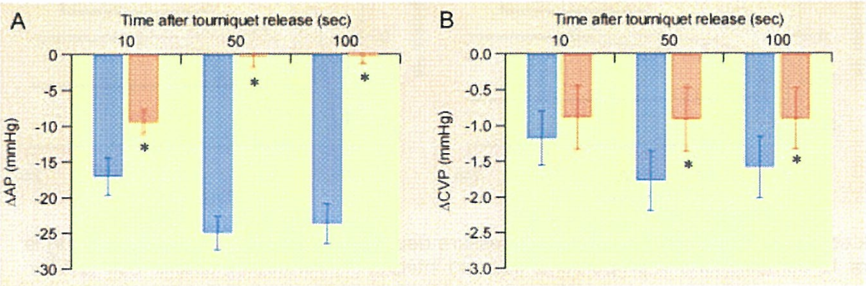

Figure 5. Bar graphs showing changes in AP (A) and CVP (B) at 10, 50, and 100 seconds after tourniquet release. Implementation of the BBS (red column) significantly attenuated tourniquet-related falls (blue column) in AP and CVP. Data are expressed as mean±SD for 21 patients. *Overall $P<0.05$.

ing.[29,31] For example, tourniquet release results in a rapid increase in venous pooling in the affected limb with a subsequent decrease in venous return and cardiac output. Under general anesthesia with volatile gases such as sevoflurane,[32,33] arterial baroreflex function is inhibited, and the hemodynamic disturbance produced by the tourniquet inevitably results in abrupt hypotension. In rare instances, tourniquet deflation can also trigger fatal circulatory collapse.[29]

Despite the fact that the BBS was implemented with fixed values of feedback correction factors for all patients, the BBS successfully stabilized AP against the hemodynamic challenge induced by sudden tourniquet release (Figure 4). These data indicate that the BBS may compensate for some individual differences in the dynamic response of AP to STM.

Finally, the CVP response to STM (Figure 4) in the present study suggests that the BBS attenuated a decrease in venous return. Previous studies have demonstrated that the baroreflex-mediated vasoconstriction in the splanchnic vascular bed is a major mechanism for recruitment of venous return during head-up tilting.[23,25] Therefore, the BBS may functionally mimic the baroreflex control of venous return and control of AP.

Study Limitations

This study possessed several limitations. First, based on the previous results[20–22] obtained from animal studies, the stimulation electrodes were placed in the epidural space at the level of the lower thoracic cord; however, further study to determine the optimal site of electrode placement would be of benefit. Second, it is unclear whether or not the feedback controller designed in the present study is universally applicable to other cases. Although preset parameters for feedback correction were used in the present study, other approaches based on a robust control theory could yield a better result. Finally, the epidural catheter method for sympathetic nerve stimulation is associated with significant pain and discomfort. Thus, practical use of the BBS requires an appropriate method for stimulating only efferent sympathetic nerves.

Clinical Implications

The present study confirmed the efficacy of the BBS in a clinical setting and suggests that the BBS has tremendous potential as a new therapeutic modality for treatment of severe orthostatic intolerance in patients with various syndromes of central baroreflex failure, including Shy-Drager syndrome, baroreceptor deafferentation, and traumatic spinal cord injuries.

Acknowledgments

This study was supported by a Health and Labor Sciences research grant (H14-NANO-002, H16-NANO-005, H15-KOKORO-019) from the Ministry of Health, Labor, and Welfare of Japan and by a grant-in-aid for scientific research (15300165) from the Ministry of Education, Science, Sports, and Culture of Japan.

Disclosures

None.

References

1. Guyton AC, Coleman TG, Granger HJ. Circulation: overall regulation. *Ann Rev Physiol*. 1972;34:13–46.
2. Robertson D. Diagnosis and management of baroreflex failure. *Primary Cardiol*. 1995;21:37–40.
3. Sunagawa K, Sato T, Kawada T. Integrative sympathetic baroreflex regulation of arterial pressure. *Ann N Y Acad Sci*. 2001;940:314–323.
4. Ketch T, Biaggioni I, Robertson R, Robertson D. Four faces of baroreflex failure: hypertensive crisis, volatile hypertension, orthostatic tachycardia, and malignant vagotonia. *Circulation*. 2002;105:2518–2523.
5. Sato T, Kawada T, Inagaki M, Shishido T, Takaki H, Sugimachi M, Sunagawa K. New analytical framework for understanding the sympathetic baroreflex control of arterial pressure. *Am J Physiol Heart Circ Physiol*. 1999;276:H2251–H2261.
6. Shy M, Drager GA. A neurological syndrome associated with orthostatic hypotension: a clinico-pathologic study. *Arch Neurol*. 1960;3:511–527.
7. The Consensus Committee of the American Autonomic Society and the American Academy of Neurology. Consensus statement on the definition of orthostatic hypotension, pure autonomic failure, and multiple system atrophy. *Neurology*. 1996;46:1470.
8. Schatz IJ. Farewell to the "Shy-Drager syndrome." *Ann Intern Med*. 1996;125:74–75.
9. Goldstein DS, Holmes C, Cannon RO III, Eisenhofer G, Kopin IJ. Sympathetic cardioneuropathy in dysautonomias. *N Engl J Med*. 1997;336:696–702.
10. Onrot J, Wiley RG, Fogo A, Biaggioni I, Robertson D, Hollister AS. Neck tumour with syncope due to paroxysmal sympathetic withdrawal. *J Neurol Neurosurg Psychiatry*. 1987;50:1063–1066.
11. Lee HT, Brown J, Fee WE Jr. Baroreflex dysfunction after nasopharyngectomy and bilateral carotid isolation. *Arch Otolaryngol Head Neck Surg*. 1997;123:434–437.
12. Frankel HL, Mathias CJ. Severe hypertension in patients with high spinal cord lesions undergoing electro-ejaculation: management with prostaglandin E_2. *Paraplegia*. 1980;18:293–299.
13. Matthews JM, Wheeler GD, Burnham RS, Malone LA, Steadward RD. The effects of surface anaesthesia on the autonomic dysreflexia response during functional electrical stimulation. *Spinal Cord*. 1997;35:647–651.
14. Wilcox CS, Puritz R, Lightman SL, Bannister R, Aminoff MJ. Plasma volume regulation in patients with progressive autonomic failure during changes in salt intake or posture. *J Lab Clin Med*. 1984;104:331–339.
15. Jordan J, Shannon JR, Diedrich A, Black B, Robertson D, Biaggioni I. Water potentiates the pressor effect of ephedra alkaloids. *Circulation*. 2004;109:1823–1825.
16. Kristinsson A. Programmed atrial pacing for orthostatic hypotension. *Acta Med Scand*. 1983;214:79–83.
17. Bannister R, da Costa DF, Hendry WG, Jacobs J, Mathias CJ. Atrial demand pacing to protect against vagal overactivity in sympathetic autonomic neuropathy. *Brain*. 1986;109:345–356.
18. Kachi T, Iwase S, Mano T, Saito M, Kunimoto M, Sobue I. Effect of L-threo-3,4-dihydroxyphenylserine on muscle sympathetic nerve activities in Shy-Drager syndrome. *Neurology*. 1988;38:1091–1094.
19. Obara A, Yamashita H, Onodera S, Yahara O, Honda H, Hasebe N. Effect of xamoterol in Shy-Drager syndrome. *Circulation*. 1992;85:606–611.
20. Sato T, Kawada T, Shishido T, Sugimachi M, Alexander J Jr, Sunagawa K. Novel therapeutic strategy against central baroreflex failure: a bionic baroreflex system. *Circulation*. 1999;100:299–304.
21. Sato T, Kawada T, Sugimachi M, Sunagawa K. Bionic technology revitalizes native baroreflex function in rats with baroreflex failure. *Circulation*. 2002;106:730–734.
22. Yanagiya Y, Sato T, Kawada T, Inagaki M, Tatewaki T, Zheng C, Kamiya A, Takaki H, Sugimachi M, Sunagawa K. Bionic epidural stimulation restores arterial pressure regulation during orthostasis. *J Appl Physiol*. 2004;97:984–990.
23. Hainsworth R, Karim F. Responses of abdominal vascular capacitance in the anaesthetized dog to changes in carotid sinus pressure. *J Physiol Lond*. 1976;262:659–677.

24. Carneiro JJ, Donald DE. Blood reservoir function of dog spleen, liver, and intestine. *Am J Physiol Heart Circ Physiol.* 1977;232:H67–H72.
25. Minson CT, Wladkowski SL, Pawelczyk JA, Kenney WL. Age, splanchnic vasoconstriction, and heat stress during tilting. *Am J Physiol Regul Integr Comp Physiol.* 1999;276:R203–R212.
26. Marmarelis PZ, Marmarelis VZ. *Analysis of Physiological Systems: The White-Noise Approach.* New York, NY: Plenum; 1978.
27. Kawada T, Sunagawa G, Takaki H, Shishido T, Miyano H, Miyashita H, Sato T, Sugimachi M, Sunagawa K. Development of a servo-controller of heart rate using treadmill. *Jpn Circ J.* 1999;63:945–950.
28. Shimoji K, Hokari T, Kano T, Tomita M, Kimura R, Watanabe S, Endoh H, Fukuda S, Fujiwara N, Aida S. Management of intractable pain with percutaneous epidural spinal cord stimulation: differences in pain-relieving effects among diseases and sites of pain. *Anesth Analg.* 1993;77:110–116.
29. Kahn RL, Marino V, Urquhart B, Sharrock NE. Hemodynamic changes associated with tourniquet use under epidural anesthesia for total knee arthroplasty. *Reg Anesth.* 1992;17:228–232.
30. Feldman DL, Wigod M, Barwick W, Levin LS. Tourniquet-related hypotension in venous stasis ulcer excision. *Ann Plast Surg.* 1993:30: 556–559.
31. Sander-Jensen K, Mehlsen J, Secher NH, Bach FW, Bie P, Giese J, Schwartz TW, Trap-Jensen J, Warberg J. Progressive central hypovolaemia in man–resulting in a vasovagal syncope? Haemodynamic and endocrine variables during venous tourniquets of the thighs. *Clin Physiol.* 1987;7:231–242.
32. Tanaka M, Nishikawa T. Arterial baroreflex function in humans anaesthetized with sevoflurane. *Br J Anaesth.* 1999;82:350–354.
33. Keyl C, Schneider A, Hobbhahn J, Bernardi L. Sinusoidal neck suction for evaluation of baroreflex sensitivity during desflurane and sevoflurane anesthesia. *Anesth Analg.* 2002;95:1629–1636.

CLINICAL PERSPECTIVE

Central baroreflex failure due to Shy-Drager syndrome, baroreceptor deafferentation, and traumatic spinal cord injuries results in severe orthostatic hypotension. However, most commonly used interventions, such as salt loading, cardiac pacing, and pharmacological approaches, can neither restore nor reproduce the functioning of a native vasomotor center. Here, we proposed a novel therapeutic strategy against central baroreflex failure and developed a bionic baroreflex system (BBS). The BBS consisted of a pressure sensor, computer, electrical stimulator, and epidural catheter with sympathetic nerve stimulation electrodes. While automatically calculating the frequency of a pulse train in response to a change in arterial pressure, the computer drove the stimulator at the appropriate frequency to stabilize arterial pressure against an external disturbance. According to a parametric negative-feedback control theory, we designed an algorithm of the computer functioning as an artificial vasomotor center. The efficacy of the BBS was tested in a clinical model of orthostatic hypotension during knee joint surgery. Without the implementation of the BBS, a sudden deflation of a thigh tourniquet resulted in rapid progressive hypotension. By contrast, during real-time execution of the BBS, arterial pressure was quickly restored to the baseline level before tourniquet release. These results suggest the technical feasibility of functional restoration of arterial baroreflex with the BBS.

J Appl Physiol 100: 1278–1286, 2006.
First published December 22, 2005; doi:10.1152/japplphysiol.01206.2005.

TRANSLATIONAL PHYSIOLOGY

Automated drug delivery system to control systemic arterial pressure, cardiac output, and left heart filling pressure in acute decompensated heart failure

Kazunori Uemura,[1] Atsunori Kamiya,[1] Ichiro Hidaka,[1] Toru Kawada,[1] Shuji Shimizu,[1] Toshiaki Shishido,[1] Makoto Yoshizawa,[2] Masaru Sugimachi,[1] and Kenji Sunagawa[3]

[1]*Department of Cardiovascular Dynamics, National Cardiovascular Center Research Institute, Suita;* [2]*Research Division on Advanced Information Technology, Information Synergy Center, Tohoku University, Sendai;* [3]*Department of Cardiovascular Medicine, Kyushu University Graduate School of Medical Science, Fukuoka, Japan*

Submitted 22 September 2005; accepted in final form 17 December 2005

Uemura, Kazunori, Atsunori Kamiya, Ichiro Hidaka, Toru Kawada, Shuji Shimizu, Toshiaki Shishido, Makoto Yoshizawa, Masaru Sugimachi, and Kenji Sunagawa. Automated drug delivery system to control systemic arterial pressure, cardiac output, and left heart filling pressure in acute decompensated heart failure. *J Appl Physiol* 100: 1278–1286, 2006. First published December 22, 2005; doi:10.1152/japplphysiol.01206.2005.—Pharmacological support with inotropes and vasodilators to control decompensated hemodynamics requires strict monitoring of patient condition and frequent adjustments of drug infusion rates, which is difficult and time-consuming, especially in hemodynamically unstable patients. To overcome this difficulty, we have developed a novel automated drug delivery system for simultaneous control of systemic arterial pressure (AP), cardiac output (CO), and left atrial pressure (Pla). Previous systems attempted to directly control AP and CO by estimating their responses to drug infusions. This approach is inapplicable because of the difficulties to estimate simultaneous AP, CO, and Pla responses to the infusion of multiple drugs. The circulatory equilibrium framework developed previously (Uemura K, Sugimachi M, Kawada T, Kamiya A, Jin Y, Kashihara K, and Sunagawa K. *Am J Physiol Heart Circ Physiol* 286: H2376–H2385, 2004) indicates that AP, CO, and Pla are determined by an equilibrium of the pumping ability of the left heart (S_L), stressed blood volume (V), and systemic arterial resistance (R). Our system directly controls S_L with dobutamine, V with dextran/furosemide, and R with nitroprusside, thereby controlling the three variables. We evaluated the efficacy of our system in 12 anesthetized dogs with acute decompensated heart failure. Once activated, the system restored S_L, V, and R within 30 min, resulting in the restoration of normal AP, CO, and Pla. Steady-state deviations from target values were small for AP [4.4 mmHg (SD 2.6)], CO [5.4 ml·min^{-1}·kg^{-1} (SD 2.4)] and Pla [0.8 mmHg (SD 0.6)]. In conclusion, by directly controlling the mechanical determinants of circulation, our system has enabled simultaneous control of AP, CO, and Pla with good accuracy and stability.

computers; negative feedback; circulatory equilibrium

IN THE MANAGEMENT OF PATIENTS with acute decompensated heart failure after myocardial infarction or after cardiac surgical procedures, cardiovascular agents such as inotropes and/or vasodilators are commonly used to control systemic arterial pressure (AP), cardiac output (CO), and left heart filling pressure (2, 13, 20). Because responses to these agents vary between patients and within patient over time, strict monitoring of patient condition and frequent adjustments of drug infusion rates are usually required. This is a difficult and time-consuming process, especially in hemodynamically unstable patients. Several closed-loop systems to automate drug infusion have been developed to facilitate this process (10, 11, 18, 26, 27). Closed-loop control of AP with vasodilators was more precise and stable than manual controls (10, 11). Chitwood et al. (10) demonstrated that, compared with manual control, closed-loop control of postoperative hypertension significantly improves patient outcome by reducing the transfusion requirement and postoperative blood loss. Although closed-loop control of hemodynamics has been suggested to be useful in clinical settings, no closed-loop system so far developed is capable of controlling the overall hemodynamics; i.e., controlling AP, CO, and left heart filling pressure simultaneously (18). This is because all previous systems attempted to directly control the hemodynamic variable by estimating response of the variable to drug infusion (10, 11, 18, 26, 27). Although such an approach worked well in controlling a single variable, it cannot be applied to control of the three variables, because it is difficult to simultaneously estimate their responses to the infusions of multiple drugs.

In this study, we developed a new automated drug delivery system that is capable of controlling AP, CO, and left atrial pressure (Pla). We modeled the entire cardiovascular system by extending Guyton's framework of circulatory equilibrium (16, 17, 24, 25). As shown in Fig. 1, the extended framework consists of an integrated cardiac output curve characterizing the pumping ability of the left and the right heart and a venous return surface characterizing the venous return property of the systemic and pulmonary circulation (24, 25). The intersection point of the integrated CO curve and the venous return surface predicts the equilibrium point of CO, Pla, and right atrial pressure (Pra) (Fig. 1) (24, 25). Once CO, Pla, and Pra are predicted from the intersection point, systemic arterial resistance determines AP. On the basis of this framework, instead of directly controlling AP, CO, and Pla, our system controls the integrated CO curve with dobutamine (Dob), the venous return surface with 10% dextran 40 (Dex) and furosemide (Fur), and systemic arterial resistance with sodium nitroprusside (SNP), thereby controlling the three hemodynamic variables.

Address for reprint requests and other correspondence: K. Uemura, Dept. of Cardiovascular Dynamics, National Cardiovascular Center Research Institute, 5-7-1 Fujishirodai, Suita 565-8565, Japan (e-mail: kuemura@ri.ncvc.go.jp).

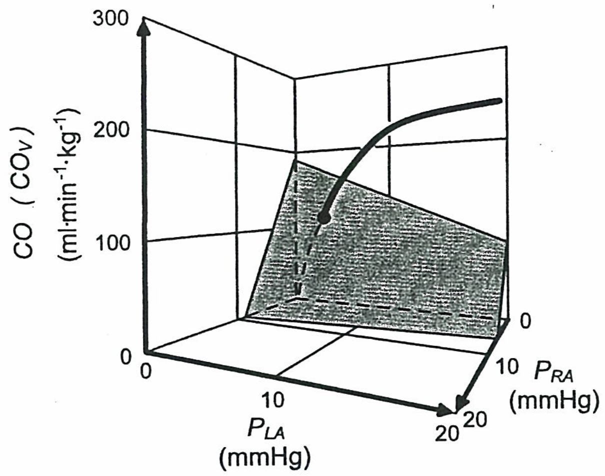

Fig. 1. Diagram of circulatory equilibrium for cardiac output (CO), venous return (CO$_V$), left atrial pressure (Pla), and right atrial pressure (Pra). The equilibrium CO, Pla, and Pra are obtained as the intersection point of the venous return surface and integrated cardiac output curve. [Modified from Uemura et al. (Ref 25).]

The purpose of this study was, therefore, to develop and validate the new automated drug delivery system. We evaluated the efficacy of our system in a canine model of acute ischemic heart failure. Our results indicated that this novel automated drug delivery system was able to control AP, CO, and Pla simultaneously with reasonably good accuracy and stability.

METHODS

Cardiac Output Curve, Venous Return Surface, and Arterial Resistance

On the basis of previous studies, we parameterized the integrated CO curve by the pumping ability of the left heart (S_L), the venous return surface by total stressed blood volume (V), and the systemic arterial resistance by R (see APPENDIX A) (24, 25). Our system aims to control these cardiovascular parameters to achieve target AP (AP*), target CO (CO*), and target Pla (Pla*).

Automated Drug Delivery System

Figure 2*A* illustrates a block diagram of the automated drug delivery system, using a negative feedback mechanism.

Target values of S_L (S_L*), V (V*), and R (R*) are determined according to the AP*, CO*, and Pla* (see APPENDIX B). The subject's S_L, V, and R are calculated from the measured AP, CO, Pla, and Pra (Fig. 2*A*). S_L, V, and R are compared with S_L*, V*, and R*, respectively.

To minimize the difference between S_L* and S_L ($\Delta S_L = S_L^* - S_L$) and the difference between R* and R ($\Delta R = R^* - R$), proportional-integral (PI) feedback controllers adjusts infusion rates of Dob and SNP, respectively (Fig. 2*A*). In the PI controller (Fig. 2*B*), ΔS_L (or ΔR) and the difference integrated with an integral gain (K_i) are summed and scaled by a proportional gain (K_p) to give the infusion rate of Dob (or SNP). We determined values of K_i and K_p on the

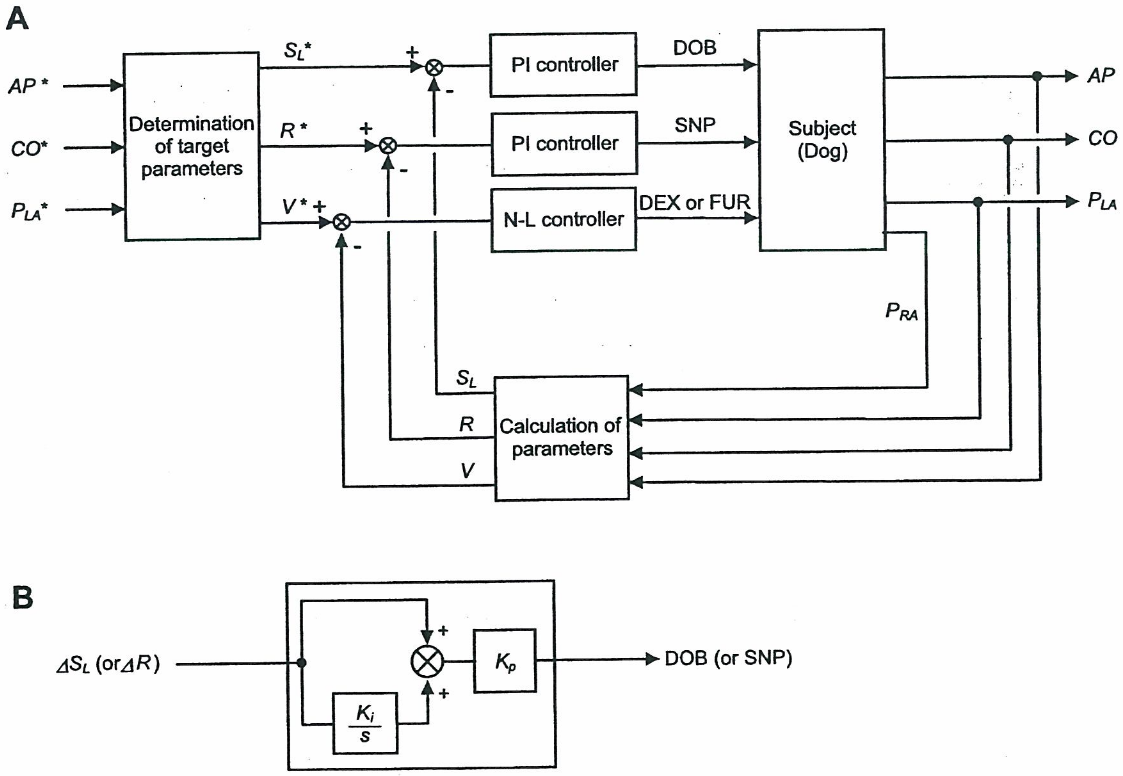

Fig. 2. *A*: block diagram of an automated drug delivery system for simultaneous control of systemic arterial pressure (AP), CO, and Pla. AP*, CO* and Pla* represent target AP, target CO, and target Pla, respectively. From these target variables, target values of pumping ability of the left heart (S_L*), stressed blood volume (V*), and systemic arterial resistance (R*) are determined. Subject's S_L, V, and R are calculated from measured AP, CO, Pla, and Pra. Proportional-integral (PI) controllers adjust infusion rate of dobutamine (Dob) and sodium nitroprusside (SNP) to minimize the difference between S_L and S_L* (ΔS_L), and the difference between R and R* (ΔR), respectively. Nonlinear (N-L) controller adjusts infusion of 10% dextran 40 (Dex) or injection of furosemide (Fur) so that the difference between V and V* is minimized. *B*: block diagram of the PI controller. K_i and K_p represent the integral and proportional gain constants, respectively; s is a Laplace operator.

basis of open-loop response of S_L (or R) to the infusion of Dob (or SNP) (4, 9).

To minimize the difference between V* and V ($\Delta V = V^* - V$), a nonlinear (NL) feedback controller (Fig. 2A) adjusts the infusion of Dex or injection of Fur on the basis of the following "if-then" rules:

Rule 1: If $\Delta V \geq X_1$ ml/kg then infuse Dex (Y_1, ml/min)

Rule 2: If $\Delta V \leq X_2$ ml/kg then inject Fur (Y_2, mg)

We determined values of X_1, Y_1, X_2, and Y_2 on the basis of the open-loop response of V to the infusion of Dex and Fur.

These adjustment processes are repeated in parallel and continued until the differences disappear.

Preparation

We used 35 adult mongrel dogs in this study [both sexes, body weight 25 kg (SD 4)]. Care of the animals was in strict accordance with the guiding principles of the Physiological Society of Japan. All protocols were approved by the Animal Subjects Committee of the National Cardiovascular Center. Anesthesia was induced with pentobarbital sodium (25 mg/kg). Animals were intubated endotracheally. Isoflurane (1.0%) was inhaled continuously to maintain an appropriate level of anesthesia during the experiment. A catheter (8-Fr) was placed in the right femoral artery, which was connected to a pressure transducer (DX-200, Nihon Kohden, Tokyo, Japan) to measure AP. After a median sternotomy, a small pericardial incision was made at the level of the aortic root. Through the incision, an ultrasonic flow meter (20A594, Transonics, Ithaca, NY) was placed around the ascending aorta to measure CO. Fluid-filled catheters were placed in the left and right atria to measure Pla and Pra, respectively. They were connected to pressure transducers (DX-200, Nihon Kohden). The junction between the vena cavae and the right atrium was taken as the reference point for zero pressure. The undamped natural frequency and the damping ratio of the fluid filled catheters for the pressure measurements were 21 Hz and 0.22, respectively. A urinary catheter was inserted to measure urine volume.

A catheter (6-Fr) was placed in the right femoral vein. A roller pump (Minipuls 3, Gilson, Middleton, WI) was attached to the venous line to infuse Dex. A double-lumen catheter was also introduced into the right femoral vein for administration of Dob and SNP. Infusion pumps (CFV-3200, Nihon Kohden) were used for Dob and SNP infusion. The infusion rates of Dex, Dob, and SNP were controlled with a personal computer (MA20V, NEC, Tokyo, Japan) through a 12-bit digital-to-analog converter (DA12-8PCI, Contec, Osaka, Japan). A catheter (6-Fr) was placed in the right external jugular vein, from which Fur was injected after a command signal from the computer.

Experimental Protocols

We induced left ventricular failure (LVF) in all the animals by embolizing the left circumflex coronary artery with glass microspheres (90 μm in diameter) (24, 25). We adjusted the amount of injected microspheres to increase Pla to more than 18 mmHg or decrease CO to less than 70 $\text{ml}\cdot\text{min}^{-1}\cdot\text{kg}^{-1}$. When ventricular tachycardia or frequent premature ventricular contractions were noted, lidocaine (1 mg/min) was infused to suppress the arrhythmia.

Response of cardiovascular parameters to drug infusion. Under open-loop conditions, we examined the response of cardiovascular parameters to drug infusions in 21 dogs with LVF. In 10 dogs, we infused Dob in a stepwise manner at 6 $\mu\text{g}\cdot\text{kg}^{-1}\cdot\text{min}^{-1}$ for 10 min to obtain a step response of S_L. In six dogs, we infused SNP at 2 $\mu\text{g}\cdot\text{kg}^{-1}\cdot\text{min}^{-1}$ for 10 min to obtain a step response of R. In five dogs, we infused Dex at 0.4 $\text{ml}\cdot\text{min}^{-1}\cdot\text{kg}^{-1}$ for 10 min to observe the response of V. In seven dogs, we injected Fur (20 mg, bolus iv) and observed the response of V and urine volume for 50 min.

Application of the automated drug delivery system. We applied the system to the other 14 dogs with LVF. We first defined AP* (90–105 mmHg), CO* (90–100 $\text{ml}\cdot\text{min}^{-1}\cdot\text{kg}^{-1}$), and Pla* (8–12 mmHg), which were fed into the system to determine S_L*, V*, and R* (see APPENDIX B). The controllers were then activated by closing the loops. In 12 dogs (*group 1*), we observed the performance of the system over 50–60 min. In two dogs (*group* 2), we observed the performance of the system over 100–150 min to evaluate stability of the closed-loop control over a longer periods of time.

With the use of the computer, analog signals of AP, CO, Pla, and Pra were digitized at 200 Hz with a 12-bit analog-to-digital converter [AD12-16U(PCI)E, Contec, Osaka, Japan] and stored on a hard disk for offline analysis. In the closed-loop control, the digitized signals were smoothed by a low-pass filter (time constant, 10 s) and were used as the system controlled variables. The infusion rates of Dob, SNP, and Dex were also stored. Urine volume after the injection of Fur was recorded.

Data Analysis

Evaluation of the response of cardiovascular parameters and design of the controller. We described the step response of S_L and R by a transfer function of a first-order model with a transport delay. In this model, change in S_L from baseline (δS_L) in response to Dob infusion can be expressed by the following formula:

$$\delta S_L(t) = \begin{cases} G \cdot \left[1 - \exp\left(-\dfrac{t-L}{T}\right)\right] & (t \geq L) \\ 0 & (t < L) \end{cases} \qquad (1)$$

where G is static gain $[\text{ml}\cdot\text{min}^{-1}\cdot\text{kg}^{-1}(\mu\text{g}\cdot\text{kg}^{-1}\cdot\text{min}^{-1})^{-1}]$, L is transport delay (s), and T is time constant (s). Change in R from baseline (δR) in response to the SNP infusion can be expressed similarly and is characterized by G $[\text{mmHg}\cdot\text{min}\cdot\text{ml}^{-1}\cdot\text{kg}$ $(\mu\text{g}\cdot\text{kg}^{-1}\cdot\text{min}^{-1})^{-1}]$, L (s), and T (s). We estimated the parameters of the transfer function by approximating δS_L and δR to *Eq. 1* using the least square method. We averaged the parameters of the transfer function of S_L response for 10 animals and those of R response for 6 animals. The averaged parameters were used to determine the PI gain constants, K_i and K_p, in accordance with the method of Chien et al. (9). Their method provides PI constants that permit the regulated variable to respond rapidly without overshoot (4, 9).

We evaluated the change in V from baseline (δV) in response to the infusion of Dex and Fur. On the basis of δV, we determined the constants (X_1, Y_1, X_2, and Y_2) of the if-then rules.

Efficacy of the automated drug delivery system. We calculated the following indexes to evaluate the accuracy and stability of the control of AP, CO, and Pla by the new system: the time required for the hemodynamic variables to reach the acceptable ranges of the target values (±10 mmHg for AP, ±10 $\text{ml}\cdot\text{min}^{-1}\cdot\text{kg}^{-1}$ for CO, ±2 mmHg for Pla), and the standard deviations of the steady-state differences between AP and AP*, between CO and CO*, and between Pla and Pla*. Because steady states were reached within 30 min in all the variables in the present study, standard deviations were calculated from 30 min after the loop was closed.

Statistics

Group data are expressed as means (SD) unless otherwise stated. Student's paired *t*-test was used to compare hemodynamic data at baseline and after the coronary embolization. One-way ANOVA with Tukey's post hoc test was used to compare hemodynamic data before, during, and after the closed-loop control of hemodynamics. The level of statistical significance was defined as $P < 0.05$.

RESULTS

Hemodynamic data at baseline and after left circumflex coronary artery embolization are summarized in Table 1. Coronary embolization more than doubled Pla [from 7.5 (SD 1.9) to 19.4 (SD 6.2) mmHg] and halved CO [from 131.4 (SD

Table 1. *Hemodynamic data at baseline and after left circumflex coronary artery embolization*

	Baseline	Embolization
HR, beats/min	141.3 (19.5) [112.0–188.3]	146.2 (28.8) [81.4–197.9]
AP, mmHg	109.1 (18.7) [76.4–140.0]	90.9 (16.5) [66.9–135.6]*
CO, $ml \cdot min^{-1} \cdot kg^{-1}$	131.4 (40.9) [64.5–229.2]	66.8 (23.3) [30.3–121.7]*
Pla, mmHg	7.5 (1.9) [4.7–12.8]	19.4 (6.2) [7.9–34.5]*
Pra, mmHg	4.2 (1.2) [2.1–7.2]	6.0 (1.8) [3.5–9.9]*
S_L, $ml \cdot min^{-1} \cdot kg^{-1}$	54.3 (18.1) [25.2–105.9]	19.1 (7.6) [8.0–33.7]*
R, $mmHg \cdot min \cdot ml^{-1} \cdot kg$	0.9 (0.4) [0.4–1.8]	1.4 (0.5) [0.7–2.6]*
V, ml/kg	31.0 (6.6) [21.7–45.2]	32.3 (4.9) [20.6–43.7]

Values are means (SD) (n = 35 in each group). Numbers in brackets are the ranges. HR, heart rate. AP, systemic arterial pressure; CO, cardiac output; Pla, left atrial pressure; Pra, right atrial pressure; S_L, pumping ability of the left heart; R, systemic arterial resistance; V, stressed blood volume. $*P < 0.01$ vs. baseline.

40.9) to 66.8 (SD 23.3) $ml \cdot min^{-1} \cdot kg^{-1}$]. This decreased S_L to about one-third of the baseline value, which indicates substantial downward shift of the left cardiac output curve. These changes are compatible with severe LVF.

Response of Cardiovascular Parameters to Drug Infusion

Figure 3 shows the open-loop responses of cardiovascular parameters to drug infusions. Figure 3, *A* and *B*, shows the averaged time course of δS_L during Dob infusion (n = 10) and that of δR during SNP infusion (n = 6), respectively. Dob infusion increased δS_L, and SNP infusion decreased δR exponentially. The results of the fit of δS_L and δR to *Eq. 1* are summarized in Table 2. The fact that the correlation coefficients were close to unity, with a small standard error of the estimate relative to the amount of δS_L and δR, suggested that the approximation of δS_L and δR to *Eq. 1* was reasonably accurate. On the basis of the averaged parameters of the transfer function (Table 2), we determined the PI gain constants for Dob infusion [$K_i = 0.01\ s^{-1}$, $K_p = 0.06\ \mu g \cdot kg^{-1} \cdot min^{-1}\ (ml \cdot min^{-1} \cdot kg^{-1})^{-1}$] and for SNP infusion [$K_i = 0.007\ s^{-1}$, $K_p = -1.37\ \mu g \cdot kg^{-1} \cdot min^{-1}\ (mmHg \cdot min \cdot ml^{-1} \cdot kg)^{-1}$].

Figure 3*C* shows the averaged time course of δV in response to Dex infusion (n = 5). δV increased and plateaued [7.2 ml/kg (SD 2.2)] after the cessation of Dex infusion. δV at the plateau was greater than the total volume of Dex infused (4 ml/kg), suggesting transvascular fluid absorption by colloid osmotic pressure (3). Figure 3*D* shows the averaged time course of δV after a single intravenous injection of Fur (20 mg, n = 7). δV gradually decreased and reached a trough [−4.3 ml/kg (SD 3.5)] around 30 min after the Fur injection. Average urine volume was 180 ml (SD 94). On the basis of these responses, we determined the constants of the if-then rules as X_1 = 1 ml/kg, Y_1 = 10 ml/min, X_2 = −2 ml/kg, and Y_2 = 10 mg. To avoid oscillation between hypovole-

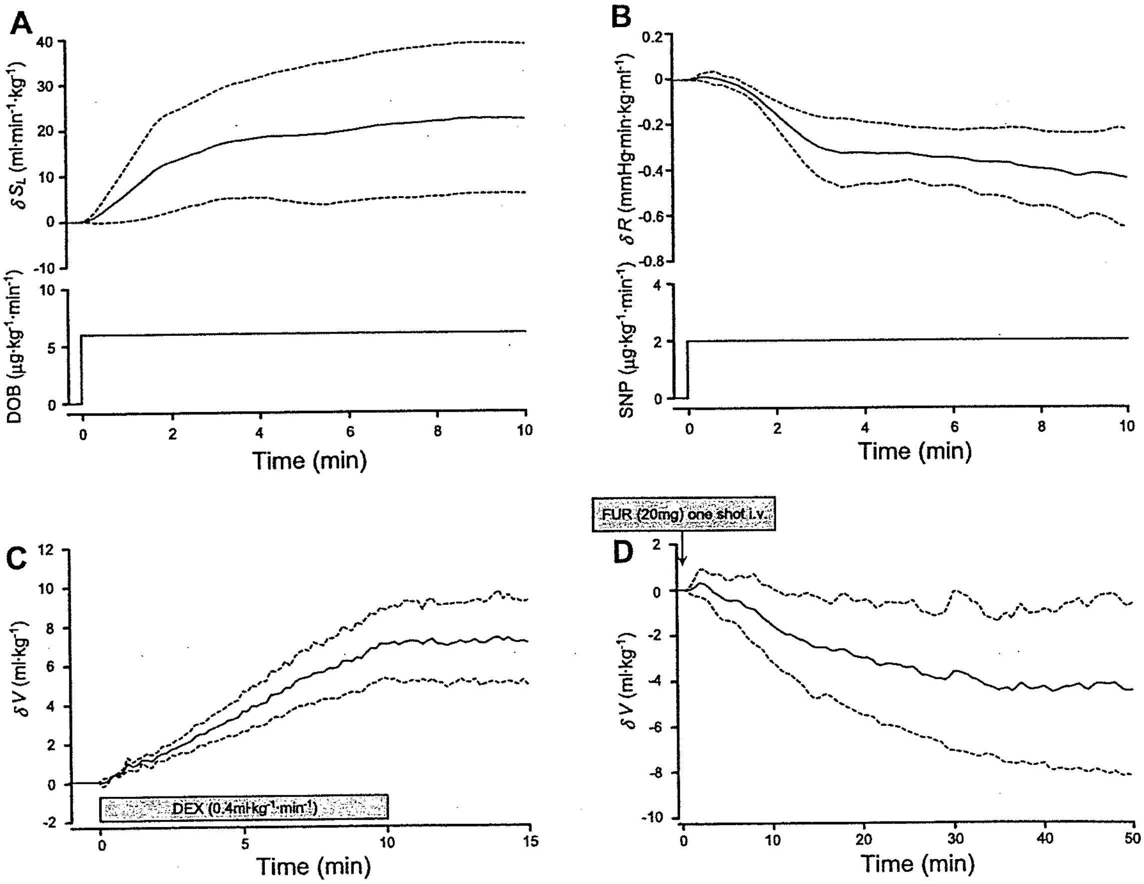

Fig. 3. Response of cardiovascular parameter to drug infusion. *A*: averaged response of S_L to stepwise Dob infusion ($6\ \mu g \cdot kg^{-1} \cdot min^{-1}$) ($n$ = 10). The ordinate indicates change in S_L from baseline (δS_L). *B*: averaged response of R to stepwise SNP infusion ($2\ \mu g \cdot kg^{-1} \cdot min^{-1}$) ($n$ = 6). The ordinate indicates change in R from baseline (δR). *C* and *D*: averaged response of V to Dex infusion ($0.4\ ml \cdot min^{-1} \cdot kg^{-1}$) (*C*, n = 5) and to Fur (20 mg) injection (*D*, n = 7). The ordinates indicate change in V from baseline (δV). Data are expressed by mean (solid line) ± SD (broken line).

Table 2. *Parameters of step response of S_L and R*

	G	L	T	r	SEE
δS_L	3.6 (2.7)	63.5 (46.9)	79.0 (78.0)	0.91 (0.09)	2.0 (0.7)
δR	−0.21 (0.08)	69.8 (26.1)	117.1 (80.2)	0.93 (0.02)	0.06 (0.02)

Values are means (SD). δS_L, change in S_L from baseline; δR, change in R from baseline; *G*, static gain of δS_L [$\mathrm{ml \cdot min^{-1} \cdot kg^{-1}}$ ($\mathrm{\mu g \cdot kg^{-1} \cdot min^{-1}})^{-1}$] and of δR [$\mathrm{mmHg \cdot min \cdot ml^{-1} \cdot kg}$ ($\mathrm{\mu g \cdot kg^{-1} \cdot min^{-1}})^{-1}$]; *L*, transport delay (s); *T*, time constant (s); *r*, correlation coefficient; SEE, standard error of the estimate of δS_L ($\mathrm{ml \cdot min^{-1} \cdot kg^{-1}}$) and of δR ($\mathrm{mmHg \cdot min \cdot ml^{-1} \cdot kg}$).

mia and hypervolemia (hence infusion of Dex and injection of Fur), we introduced a dead zone (-2 ml/kg $< \Delta V <$ 1 ml/kg) into the rules (4). We set continuous checking for *rule 1* and checking at 20-min intervals for *rule 2*.

With the controllers thus designed, we evaluated the performance of the automated system in the next protocol.

Performance of the Automated Drug Delivery System

Figure 4 shows the experimental trial in a representative case. The automated system was activated at 0 min. Figure 4*A* shows the time courses of the infusion rates of Dob and SNP and the accumulated volume of infused Dex. In this case, Fur was not injected. Figure 4*B* shows the time courses of S_L, R, and V. Infusion rates of Dob, SNP, and Dex were adjusted so that S_L, R, and V reached their respective target values. By controlling the cardiovascular parameters, the automated system controlled AP, CO, and Pla accurately and stably as demonstrated in Fig. 4*C*. AP, CO, and Pla reached their respective target levels within 30 min and remained at these levels.

Figure 5 summarizes the results obtained for 12 dogs (*group 1*), demonstrating the effectiveness of the performance of the automated system. Figure 5*A* shows averaged time courses of the infusion rates of Dob and SNP, and the accumulated volume of infused Dex. The average infusion rates of Dob and SNP were 4.7 $\mathrm{\mu g \cdot kg^{-1} \cdot min^{-1}}$ (SD 2.6) and 4.2 $\mathrm{\mu g \cdot kg^{-1} \cdot min^{-1}}$ (SD 1.8), respectively. The average volume of infused Dex was 2.4 ml/kg (SD 1.9). Fur was injected once in one animal and twice in another animal. In these two animals, V decreased by 3.8–10.2 ml/kg in response to the injection of Fur with a total urine volume of 250–300 ml. Figure 5*B* shows averaged time courses of difference between S_L and S_L* ($S_L - S_L$*), difference between R and R* (R − R*), and difference between V and V* (V − V*). Once the system was activated, these differences rapidly converged to the zero lines in all the animals. S_L was restored to subnormal conditions [33.0 $\mathrm{ml \cdot min^{-1} \cdot kg^{-1}}$ (SD 2.6)] irrespective of the magnitude of depression before the control [13.8 $\mathrm{ml \cdot min^{-1} \cdot kg^{-1}}$ (SD 3.5), from 9.4 to 20.5 $\mathrm{ml \cdot min^{-1} \cdot kg^{-1}}$]. These resulted in accurate and stable control of AP, CO, and Pla (Fig. 5*C*). The ordinates of Fig. 5*C* indicate the difference between AP and AP* (AP − AP*), difference between CO and CO* (CO − CO*), and difference between Pla and Pla* (Pla − Pla*). These differences also converged to the zero lines rapidly. The average times for AP, CO, and Pla to reach the acceptable ranges were 5.2 min (SD 6.6), 6.8 min (SD 4.6), and 11.7 min (SD 9.8),

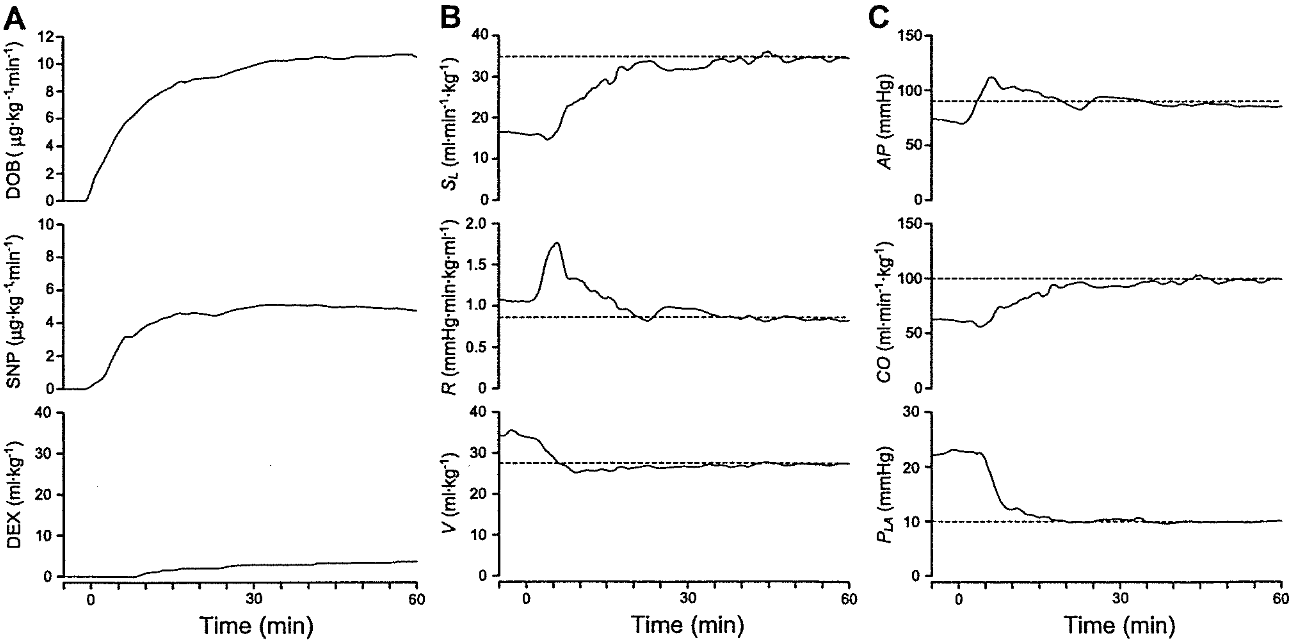

Fig. 4. Time courses of infusion rates of Dob and SNP, and cumulated volume of infused Dex (*A*), cardiovascular parameters (*B*), and hemodynamic variables (*C*) in 1 representative animal during closed-loop control of hemodynamics. Broken horizontal lines in *B* indicate target parameters (*top*, S_L*; *middle*, R*; *bottom*, V*). Broken horizontal lines in *C* indicate target hemodynamic variables (*top*, AP*; *middle*, CO*; *bottom*, Pla*). Drug infusion rates were adjusted so that the cardiovascular parameters reached the respective target values. As the parameters got closer to their targets, all 3 hemodynamic variables approached their respective target values.

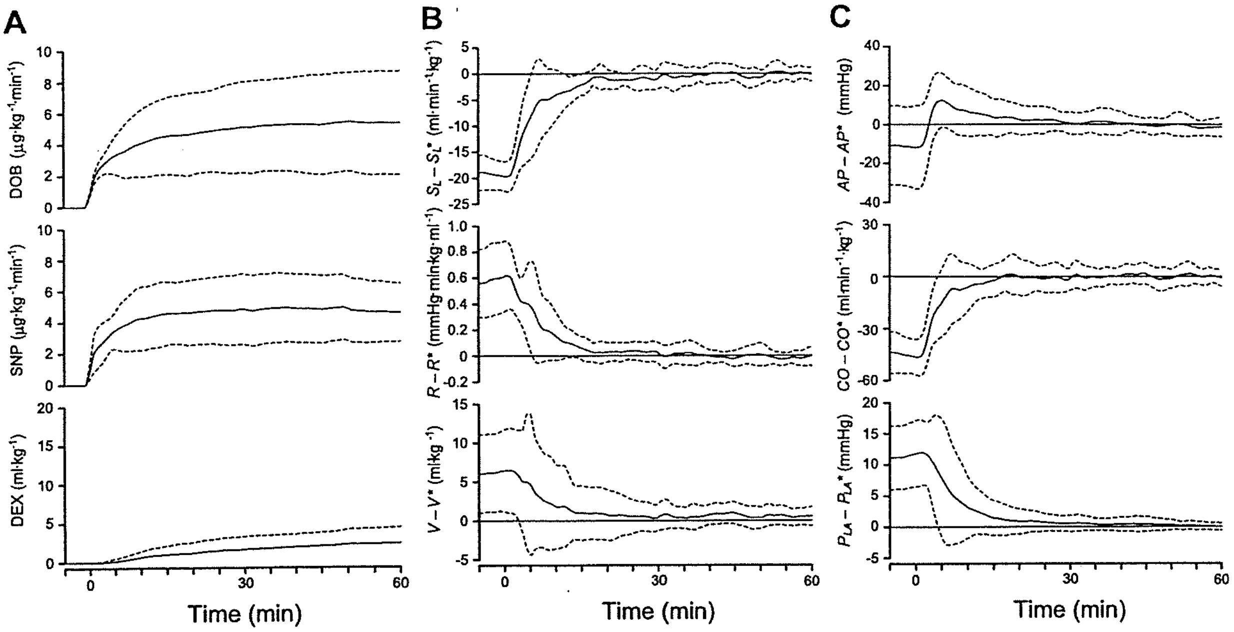

Fig. 5. Time courses of infusion rates of Dob and SNP, and cumulated volume of infused Dex (*A*), differences between measured and target cardiovascular parameters (*B*), and differences between measured and target hemodynamic variables (*C*) averaged for 12 dogs during closed-loop control of hemodynamics. Data are expressed as mean (solid line) ± SD (broken line). As the differences between measured and target parameters converged to the zero lines, the differences between measured and target hemodynamic variables also converged to the zero lines and remained at those levels.

respectively. The average standard deviations from the target values were small for AP [4.4 mmHg (SD 2.6)], CO [5.4 ml·min^{-1}·kg^{-1} (SD 2.4)] and Pla [0.8 mmHg (SD 0.6)]. In case of severe hypotension, restoring normal AP should be done within a few minutes to prevent cerebral ischemia. Four of 12 dogs exhibited severe hypotension [AP, 67 mmHg (SD 6)]. In these animals, AP* [95 mmHg (SD 4)] was attained within 4 min [mean 2.8 min (SD 0.7)]. Hemodynamic data before, during, and after the closed-loop control of hemodynamics are summarized in Table 3. After the system was turned off, AP, CO, and Pla gradually returned to their precontrol levels in 11 animals. In one animal, however, progressive hypotension followed by intractable ventricular fibrillation occurred ~3 min after the system was turned off.

In two dogs (*group 2*), AP, CO, and Pla were controlled with reasonable stability over a longer periods of time (100–150 min). Standard deviations from target values were small for AP (3.9–7.8 mmHg), CO (2.7–6.6 ml·min^{-1}·kg^{-1}), and Pla (0.7–2.5 mmHg).

Table 3. *Hemodynamic data before, during, and after the closed-loop control of hemodynamics*

	Before (n = 12)	During (n = 12)	After (n = 11)
HR, beats/mm	147.4 (26.8)	149.4 (25.0)	135.7 (25.2)†‡
AP, mmHg	86.7 (22.4)	97.0 (7.4)	75.2 (21.1)‡
CO, ml·min^{-1}·kg^{-1}	53.7 (14.6)	96.7 (5.3)†	53.5 (8.6)‡
Pla, mmHg	21.8 (5.5)	10.8 (1.2)†	18.5 (3.4)‡
Pra, mmHg	6.9 (1.8)	4.4 (0.9)†	7.4 (2.2)‡
S$_L$, ml·min^{-1}·kg^{-1}	14.3 (4.0)	32.7 (2.6)†	15.1 (2.9)‡
R, mmHg·min·ml^{-1}·kg	1.5 (0.3)	1.0 (0.1)†	1.3 (0.4)*‡
V, ml/kg	34.2 (4.9)	28.5 (2.3)†	34.0 (5.4)‡

Values are means (SD). *$P < 0.05$, †$P < 0.01$ vs. Before; ‡$P < 0.01$ vs. During.

DISCUSSION

To the best of our knowledge, the automated drug delivery system we have developed is the first to successfully control AP, CO, and Pla simultaneously with reasonably good accuracy and stability. In a canine model of acute heart failure, our system automatically normalizes AP, CO, and Pla and maintains the levels stably within the desired ranges. Therefore, our system is potentially useful in the management of patients with acute decompensated heart failure.

Previous Closed-Loop Systems Controlling Hemodynamic Variables

Several previous systems have attempted to control two hemodynamic variables simultaneously (18, 26, 27). However, it is difficult to expand them to closed-loop control of the overall hemodynamics.

Voss et al. (26) and Yu et al. (27) reported closed-loop systems to control AP and CO using inotropes and vasodilators in dogs. In these systems, all possible input-output relations between drug infusion and the response of the controlled variable have to be estimated; namely, inotrope-AP, inotrope-CO, vasodilator-AP, and vasodilator-CO relations. The reason for this is that these drugs affect AP and CO simultaneously to almost the same degree. If this approach is applied to simultaneous control of AP, CO, and Pla, at least nine input-output relations have to be estimated, because at least three drugs are required to independently control the three variables. This would make the system extremely complicated and therefore be practically unfeasible.

In addition, the input-output relations must be estimated online in individual animals to tune the drug controllers. The reason for this is that the relations differ widely between animals and within animal over time. Even the direction of the output response can change. For example, CO usually increases in response to SNP infusion in subjects with failing hearts but may also decrease in subjects with preserved cardiac function (23, 26). In the closed-loop system of Voss et al., such estimation induced unacceptably large fluctuations in AP (26). The feasibility of such online estimation is questionable when drug infusion rates are allowed to vary simultaneously because of the difficulty to differentiate between drug effects. To avoid this problem, Hoeksel et al. (18) allowed only one drug to be varied at a time, whereas other drugs were kept constant in closed-loop control of AP and pulmonary arterial pressure during cardiac surgery. However, their adjustments of volume supplementation or dobutamine infusion were manual. Their system did not completely automate the control of hemodynamics.

Characteristics of Our System

Our system controls the cardiovascular parameters characterizing the integrated CO curve, venous return surface, and arterial resistance and as a result achieves target values for hemodynamic variables. Compared with previous systems, our system may appear to adopt a rather roundabout approach. Our concept is that controlling the cardiovascular parameters is physiologically more rational, because it is equivalent to directly controlling the mechanical determinants of circulation. As indicated by Guyton et al. (16, 17), when the mechanics of the circulation are considered, the hemodynamic variables such as AP, CO, and atrial pressures are the effects, or dependent variables. Blood volume and the mechanical properties of the heart and vasculature, such as heart rate, ventricular contractility, and vascular resistance, are the causes, or independent variables. The integrated CO curve and venous return surface display these properties through the relationship between the flow and atrial pressures (24, 25). The total artificial heart control system developed by Abe et al. (1) adjusted its output in accordance with the vascular conductance (1/resistance) and AP, thereby achieving appropriate response to peripheral metabolic demands and avoiding hemodynamic abnormalities exhibited by other total artificial heart control systems. Their results also suggest that it is essential to consider the mechanical determinant of circulation for the control of the hemodynamic variables.

Our approach is advantageous from the perspective of control engineering. The three drug controllers (Fig. 2*A*) are designed on the basis of only four input-output relations between the drug infusion and the response of the controlled parameter; namely, Dob-S_L, SNP-R, Dex-V, and Fur-V (Fig. 3). We also found that Dob decreases R and increases V, and SNP increases S_L and decreases V (data not shown), which are compatible with previous studies (7, 22, 23). If these secondary effects induce significant interactions among the three closed loops, additional controllers would be needed to compensate for the interactions (4). However, our results indicate that these secondary effects are small enough to be compensated by the three drug controllers, and additional controllers are not necessary. The fact that the three closed loops are effectively decoupled drastically simplifies the entire system. This also permits system operators to understand its behavior easily (4).

Although we fix the PI gain constants and the constants of if-then rules, controls of cardiovascular parameters are accurate and stable (Fig. 4*B*). There are interindividual differences in the response of the parameters to drug infusion (Fig. 3). There should also be intraindividual differences in the response over time. However, our results indicate that the three drug controllers effectively compensate for all of these differences and do not require adaptive tuning in individual animals as in the previous system. As long as each cardiovascular parameter responds sensitively to the corresponding agent, our system is able to achieve target values for all the parameters, thereby achieving target hemodynamic variables.

Our system explicitly quantifies cardiac pump function, preload, and afterload, thereby controlling the overall hemodynamics. We believe that this unique feature of our system is intuitively appealing and is acceptable to clinicians.

Clinical Application of Our System

Our system will reduce the stress and work imposed on physicians and nurses who are managing patients with unstable hemodynamic conditions. These personnel will be able to spend more time on other patient-related activities, thereby improving the quality of patient care (10, 11). We believe that the closed-loop control of overall hemodynamics can extend the improvement in postoperative outcome demonstrated by Chitwood et al. (10) to various aspects of clinical cardiology or cardiac surgery.

In clinical settings, multisystem disorders such as renal disease, anemia, and diabetes may affect the performance of our system. Renal disease can weaken the response of V to the infusion of Fur. The hemodynamic changes in anemia include increased preload and reduced arterial resistance as compensatory mechanisms for the reduced oxygen-carrying capacity of the blood (8). These changes may affect the control of V and R by our system. In patients with diabetic cardiomyopathy, the sensitivity of S_L to Dob infusion may be reduced (5). Drugs prescribed before hospitalization such as β-blockers, or used during hospitalization such as morphine may also affect the performance of our system. Chronic β-adrenergic blockade can weaken the sensitivity of S_L to Dob infusion (2). Administration of morphine may change the response of V and R to the drugs infused (15). We must clarify these effects on the performance of our system as thoroughly as possible before our system can be considered for clinical application.

In the routine clinical environment, CO, and pulmonary artery occlusion pressure, a substitute for Pla, are measured intermittently with a Swan-Ganz catheter. For clinical application of our system, it is a prerequisite to monitor these variables continuously. Several methods have been developed to continuously monitor CO or the pulmonary artery occlusion pressure (6, 12). Integrating these methods into our system would bring the clinical application of our system closer to reality.

Limitations

All the experiments of this study were conducted in anesthetized, open-chest dogs. Anesthesia and surgical trauma affect the cardiovascular system significantly. Whether the present system is efficacious in conscious, closed-chest animals (including humans) remains to be seen.

We parameterized the integrated cardiac output curve and the venous return surface using *Eqs. A1*, *A2*, and *A4* (24, 25). Even if the actual curve or surface deviate slightly from those estimated by these equations, our system compensates such deviations by the negative feedback mechanism. However, we did not confirm whether the estimation works well outside the physiological ranges of Pla and Pra, particularly under low atrial pressures (24, 25). The efficacy of our system in such conditions remains to be evaluated.

Our system controls R with vasodilators only and lacks a controller to increase R with vasoconstrictors. This will not be a major problem because the pathophysiology of acute heart failure is characterized by excessive vasoconstriction due to enhanced activity of sympathetic and renin-angiotensin systems (19). Vasoconstrictor control is necessary, however, for the management of patients with excessive vasodilatation, such as those in septic shock (21).

In this study, control of S_L was accurate and stable. However, it would be impossible to restore S_L pharmacologically if S_L is more severely depressed than those seen in this study as in the case of more diffuse myocardial disease or superimposed coronary artery disease. We must clarify in future studies to what magnitude of S_L depression can our system restore it reliably. In addition, how to use our system with mechanical circulatory support such as the intra-aortic balloon pump in case of the severe S_L depression remains to be established.

In the present design, if S_L is unable to respond to the infusion of Dob, the system will automatically increase the infusion rate of Dob owing to its negative feedback mechanism. This would be problematic especially in case of arrhythmia, which is a serious noise in the closed-loop control of S_L. If not appropriately suppressed, frequent premature ventricular contractions or ventricular tachycardia will depress S_L owing to disorganized ventricular contraction. In response to the depressed S_L, the system automatically increases the infusion rate of dobutamine. This could further exacerbate the arrhythmia, thus leading to a vicious cycle and collapse of the hemodynamics. To prevent such malfunction, a smart "sensor" that will filter these unwanted artifacts should be included in our system.

In the present study, we recorded only the urine volume. Measurement of urine flow and sodium excretion is essential to evaluate renal function, which is a very important prognostic indicator in patients with acute decompensated heart failure (14). It would be desirable to add the monitoring of these parameters to our system to improve the quality of patient care.

In conclusion, by directly controlling the mechanical determinants of circulation, our automated drug delivery system allows simultaneous control of AP, CO, and Pla with reasonable accuracy and stability and is potentially a powerful clinical tool for the management of patients with acute decompensated heart failure.

APPENDIX A

Parameters of Integrated Cardiac Output Curve, Venous Return Surface, and Arterial Resistance

We parameterized the integrated CO curve, the venous return surface and the systemic arterial resistance on the basis of previous studies (24, 25). In the integrated CO curve, CO ($\mathrm{ml \cdot min^{-1} \cdot kg^{-1}}$) is closely related to Pla (mmHg) by the following formula (24):

$$\mathrm{CO} = S_L \times [\ln(\mathrm{Pla} - 2.03) + 0.80] \qquad (A1)$$

and CO to Pra (mmHg) as follows:

$$\mathrm{CO} = S_R \times [\ln(\mathrm{Pra} - 1.0) + 0.88] \qquad (A2)$$

S_L and S_R ($\mathrm{ml \cdot min^{-1} \cdot kg^{-1}}$) are parameters representing the preload sensitivity of CO, i.e., the pumping ability of the left and right heart, respectively. These relations are consistent among different animals (24). In a preliminary study, we found that the ratio of S_R to S_L (α) remains fairly constant during infusion of dobutamine (data not shown). This suggests that once we know α, we can predict S_R in relation to a known change in S_L. Therefore we used S_L to parameterize the integrated CO curve. S_L can be calculated from CO and Pla by rewriting *Eq. A1* as follows:

$$S_L = \mathrm{CO}/[\ln(\mathrm{Pla} - 2.03) + 0.80] \qquad (A3)$$

The venous return surface can be mathematically expressed by the following formula (25):

$$\mathrm{CO_V} = \mathrm{V}/0.129 - 19.61\mathrm{Pra} - 3.49\mathrm{Pla} \qquad (A4)$$

V (ml/kg) is total stressed blood volume, and $\mathrm{CO_V}$ ($\mathrm{ml \cdot min^{-1} \cdot kg^{-1}}$) is integrated venous return from systemic and pulmonary circulations. This relationship is also consistent among different animals (25). We used V to parameterize the venous return surface. V can be calculated from CO (= $\mathrm{CO_V}$), Pla, and Pra by rewriting *Eq. A4* as follows:

$$\mathrm{V} = (\mathrm{CO} + 19.61\mathrm{Pra} + 3.49\mathrm{Pla}) \times 0.129 \qquad (A5)$$

We parameterized the systemic arterial resistance (R) ($\mathrm{mmHg \cdot ml^{-1} \cdot min \cdot kg}$) by the following formula:

$$\mathrm{R} = (\mathrm{AP} - \mathrm{Pra})/\mathrm{CO} \qquad (A6)$$

APPENDIX B

Determination of Target Parameters

On the basis of AP*, CO*, and Pla*, our system determines S_L*, V*, and R* as follows: S_L* is calculated by substituting CO* and Pla* into *Eq. A3*. By substituting baseline CO, Pla, and Pra into *Eqs. A1* and *A2*, baseline S_L and S_R are calculated to determine α. S_R (S_R*) corresponding to S_L* is predicted as:

$$S_R{}^* = \alpha \cdot S_L{}^* \qquad (B1)$$

From *Eq. A2* and *B1*, target Pra (Pra*) is predicted as:

$$\mathrm{Pra}^* = \exp[(\mathrm{CO}^*)/(S_R{}^*) - 0.88] + 1.0 \qquad (B2)$$

By substituting CO*, Pla*, and Pra* into *Eq. A5*, V* can be determined. By substituting AP*, CO*, and Pra* into *Eq. A6*, R* can be calculated.

GRANTS

This study was supported by Grant-in-Aid for Young Scientists (B) (16700379) from the Ministry of Education, Culture, Sports, Science and Technology, by Health and Labour Sciences Research Grants for Research on Medical Devices for Analyzing, Supporting and Substituting the Function of Human Body (H15-physi-001) from the Ministry of Health Labour and Welfare of Japan, and by the Program for Promotion of Fundamental Studies in Health Science of the National Institute of Biomedical Innovation. This study was also conducted as a part of "Ground-based Research Announcement for Space Utilization" promoted by Japan Space Forum.

REFERENCES

1. **Abe Y, Chinzei T, Mabuchi K, Snyder AJ, Isoyama T, Imanishi K, Yonezawa T, Matsuura H, Kouno A, Ono T, Atsumi K, Fujimasa I, and Imachi K.** Physiological control of a total artificial heart: conductance- and arterial pressure-based control. *J Appl Physiol* 84: 868–876, 1998.
2. **Antman EM, Anbe DT, Armstrong PW, Bates ER, Green LA, Hand M, Hochman JS, Krumholz HM, Kushner FG, Lamas GA, Mullany CJ, Ornato JP, Pearle DL, Sloan MA, and Smith SC Jr; American College of Cardiology; American Heart Association; Canadian Car-

diovascular Society. ACC/AHA guidelines for the management of patients with ST-elevation myocardial infarction—executive summary. A report of the American College of Cardiology/American Heart Association Task Force on Practice Guidelines (Writing Committee to revise the 1999 guidelines for the management of patients with acute myocardial infarction). *J Am Coll Cardiol* 44: 671–719, 2004.

3. **Arakawa M, Jerome EH, Enzan K, Grady M, and Staub NC.** Effects of dextran 70 on hemodynamics and lung liquid and protein exchange in awake sheep. *Circ Res* 67: 852–861, 1990.
4. **Astrom KJ and Hagglund T.** *PID Controller: Theory, Design, and Tuning* (2nd ed.). Research Triangle Park, NC: Instrument Society of America, 1995, p. 59–199.
5. **Atkins FL, Dowell RT, and Love S.** β-Adrenergic receptors, adenylate cyclase activity, and cardiac dysfunction in the diabetic rat. *J Cardiovasc Pharmacol* 7: 66–70, 1985.
6. **Bein B, Worthmann F, Tonner PH, Paris A, Steinfath M, Hedderich J, and Scholz J.** Comparison of esophageal Doppler, pulse contour analysis, and real-time pulmonary artery thermodilution for the continuous measurement of cardiac output. *J Cardiothorac Vasc Anesth* 18: 185–189, 2004.
7. **Binkley PF, Murray KD, Watson KM, Myerowitz PD, and Leier CV.** Dobutamine increases cardiac output of the total artificial heart. Implications for vascular contribution of inotropic agents to augmented ventricular function. *Circulation* 84: 1210–1215, 1991.
8. **Chapler CK and Cain SM.** The physiologic reserve in oxygen carrying capacity: studies in experimental hemodilution. *Can J Physiol Pharmacol* 64: 7–12, 1986.
9. **Chien KL, Hrones JA, and Reswick JB.** On the automatic control of generalized passive systems. *Trans ASME* 74: 175–185, 1952.
10. **Chitwood WR Jr, Cosgrove DM III, and Lust RM.** Multicenter trial of automated nitroprusside infusion for postoperative hypertension. Titrator Multicenter Study Group. *Ann Thorac Surg* 54: 517–522, 1992.
11. **Cosgrove DM III, Petre JH, Waller JL, Roth JV, Shepherd C, and Cohn LH.** Automated control of postoperative hypertension: a prospective, randomized multicenter study. *Ann Thorac Surg* 47: 678–682, 1989.
12. **DeBoisblanc BP, Pellett A, Johnson R, Champagne M, McClarty E, Dhillon G, and Levitzky M.** Estimation of pulmonary artery occlusion pressure by an artificial neural network. *Crit Care Med* 31: 261–266, 2003.
13. **Forrester JS, Diamond G, Chatterjee K, and Swan HJ.** Medical therapy of acute myocardial infarction by application of hemodynamic subsets (first of two parts). *N Engl J Med* 295: 1356–1362, 1976.
14. **Gottlieb SS, Abraham W, Butler J, Forman DE, Loh E, Massie BM, O'Connor CM, Rich MW, Stevenson LW, Young J, and Krumholz HM.** The prognostic importance of different definitions of worsening renal function in congestive heart failure. *J Card Fail* 8: 136–141, 2002.
15. **Greenberg S, McGowan C, Xie J, and Summer WR.** Selective pulmonary and venous smooth muscle relaxation by furosemide: a comparison with morphine. *J Pharmacol Exp Ther* 270: 1077–1085, 1994.
16. **Guyton AC.** Determination of cardiac output by equating venous return curves with cardiac response curves. *Physiol Rev* 35: 123–129, 1955.
17. **Guyton AC, Coleman TG, and Granger HJ.** Circulation: overall regulation. *Annu Rev Physiol* 34: 13–46, 1972.
18. **Hoeksel SA, Blom JA, Jansen JR, Maessen JG, and Schreuder JJ.** Automated infusion of vasoactive and inotropic drugs to control arterial and pulmonary pressures during cardiac surgery. *Crit Care Med* 27: 2792–2798, 1999.
19. **Johnson W, Omland T, Hall C, Lucas C, Myking OL, Collins C, Pfeffer M, Rouleau JL, and Stevenson LW.** Neurohormonal activation rapidly decreases after intravenous therapy with diuretics and vasodilators for class IV heart failure. *J Am Coll Cardiol* 39: 1623–1629, 2002.
20. **Kaplan JA and Guffin AV.** Treatment of perioperative left ventricular failure. In: *Cardiac Anesthesia* (3rd ed.), edited by Kaplan JA. Philadelphia, PA: Saunders, 1993, p. 1058–1094.
21. **Martin C, Viviand X, Arnaud S, Vialet R, and Rougnon T.** Effects of norepinephrine plus dobutamine or norepinephrine alone on left ventricular performance of septic shock patients. *Crit Care Med* 27: 1708–1713, 1999.
22. **Ogilvie RI and Zborowska-Sluis D.** Effects of nitroglycerin and nitroprusside on vascular capacitance of anesthetized ganglion-blocked dogs. *J Cardiovasc Pharmacol* 18: 574–580, 1991.
23. **Pouleur H, Covell JW, and Ross J Jr.** Effects of nitroprusside on venous return and central blood volume in the absence and presence of acute heart failure. *Circulation* 61: 328–337, 1980.
24. **Uemura K, Kawada T, Kamiya A, Aiba T, Hidaka I, Sunagawa K, and Sugimachi M.** Prediction of circulatory equilibrium in response to changes in stressed blood volume. *Am J Physiol Heart Circ Physiol* 289: H301–H307, 2005.
25. **Uemura K, Sugimachi M, Kawada T, Kamiya A, Jin Y, Kashihara K, and Sunagawa K.** A novel framework of circulatory equilibrium. *Am J Physiol Heart Circ Physiol* 286: H2376–H2385, 2004.
26. **Voss GI, Katona PG, and Chizeck HJ.** Adaptive multivariable drug delivery: control of arterial pressure and cardiac output in anesthetized dogs. *IEEE Trans Biomed Eng* 34: 617–623, 1987.
27. **Yu C, Roy RJ, Kaufman H, and Bequette BW.** Multiple-model adaptive predictive control of mean arterial pressure and cardiac output. *IEEE Trans Biomed Eng* 39: 765–778, 1992.

ELSEVIER

International Journal of Cardiology 111 (2006) 67 – 74

International Journal of
Cardiology

www.elsevier.com/locate/ijcard

Postexercise VO_2 “Hump” phenomenon as an indicator for inducible myocardial ischemia in patients with acute anterior myocardial infarction

Hiroshi Takaki [a,*], Satoru Sakuragi [b], Noritoshi Nagaya [b], Shoji Suzuki [b], Yoichi Goto [b], Takayuki Sato [c], Kenji Sunagawa [a]

[a] *Department of Cardiovascular Dynamics, National Cardiovascular Center Research Institute, 5-7-1 Fujishiro-dai, Suita, Osaka, 565-8565, Japan*
[b] *Division of Cardiology, Department of Internal Medicine, National Cardiovascular Center, Suita, Japan*
[c] *Department of Cardiovascular Control, Kochi Medical School, Nankoku, Japan*

Received 13 October 2004; received in revised form 30 May 2005; accepted 24 July 2005

Abstract

Objectives: At exercise testing with respiratory gas analysis in patients with inducible myocardial ischemia, we have occasionally observed abnormal transient oxygen uptake (VO_2) components with a characteristic “Hump”-shaped morphology early after exercise, which may serve as an index for inducible ischemia. We examined this hypothesis in patients with anterior q-wave myocardial infarction in whom the accuracy to identify ischemia by exercise ECG is limited.

Design: From patients with acute anterior q-wave infarction but without clinically overt heart failure who underwent pre-discharge exercise testing, we examined patients with (Group-I, $n=30$) and without (Group-N, $n=29$) inducible ischemia. To identify “Hump”, postexercise VO_2 (up to 4 min) standardized for peak VO_2 was exponentially fitted with use of peak VO_2 and VO_2 of 90–240 s, yielding “expected VO_2”. “D-curve” was obtained by subtracting “expected VO_2” from measured VO_2.

Results: Although exercise-induced ST depressions more frequently appeared in Group-I (27%) than in Group-N (3%, $p<0.05$), the prevalence was low. D-curve peaked later ($p<0.01$) and its value was greater ($p<0.05$) in Group-I than in Group-N. When “Hump” was defined to be present if D-curve peaked ≥40 s and its peak value ≥15%, it was far more frequently found in Group-I ($n=17/30$) than in Group-N ($n=1/29$, $p<0.01$). Thus, “Hump” could diagnose inducible ischemia with a sensitivity of 57% and a specificity of 97%.

Conclusions: Although not highly sensitive, postexercise VO_2 “Hump” with its peak occurring around 60 s after exercise is a specific marker for inducible ischemia. The identification may be useful, particularly in patients with limited accuracy of exercise ECG such as those with q-wave anterior infarction.

Keywords: Exercise test; Respiratory gas analysis; Myocardial ischemia; Oxygen uptake

1. Introduction

In patients after acute myocardial infarction, the evaluation of inducible myocardial ischemia is important in the subsequent management, [1–3]] however, the diagnostic accuracy of exercise ECG is known to be limited in those patients [4–8]]. This is particularly crucial in patients with q-wave anterior infarction, in whom exercise-induced ST-segment depression would be often obscured by the presence of q-wave in the precordial leads.

Exercise testing with respiratory gas analysis is most often performed for evaluating the functional capacity and predicting prognosis in patients with heart failure, however, we have conducted the test in a considerable number of these post-infarct patients (approximately 200 tests/year) in our institute for more than 10 years [9]. Although the concomitant use of respiratory gas analysis is conducted mainly for the same purpose as above, postexercise oxygen uptake (VO_2) kinetics may provide useful information for detecting inducible ischemia in these patients. In practice,

---

[*] Corresponding author. Tel.: +81 6 6833 5012; fax: +81 6 6835 5403.
E-mail address: htakaki@res.ncvc.go.jp (H. Takaki).

0167-5273/$ - see front matter
doi:10.1016/j.ijcard.2005.07.012